AD-A040 583 RCA GOVERNMENT SYSTEMS DIV MOORESTOWN N J MISSILE AND--ETC F/G 17/9
DUAL-BAND MONOPULSE ANTENNA TRACKING SYSTEM.(U)
MAR 76 N00014-75-C-0500
UNCLASSIFIED NL

1 OF 1
AD
A040583

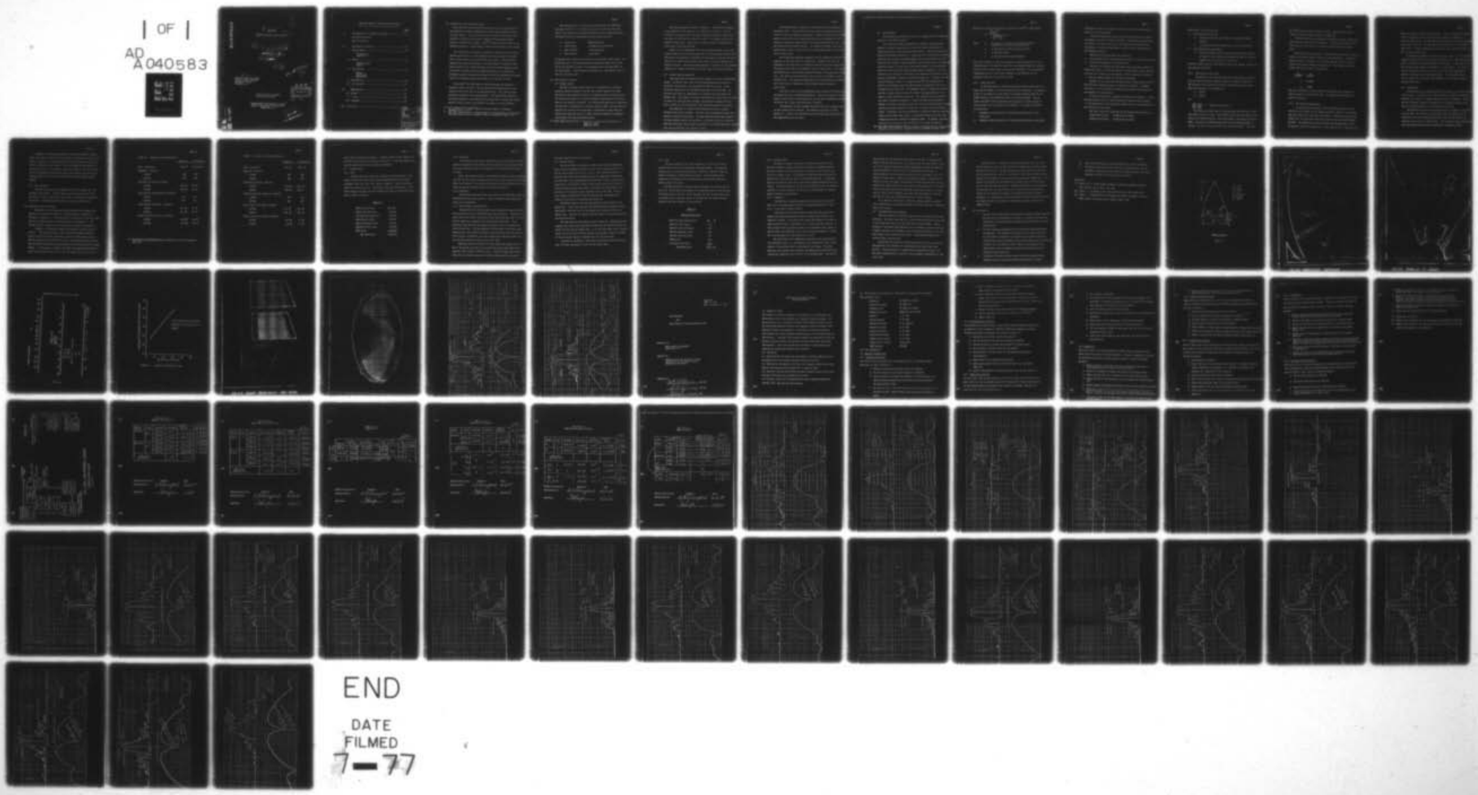

END
DATE
FILMED
7-77

(1)

B.S.

(6) DUAL-BAND

MONOPULSE ANTENNA TRACKING SYSTEM.

(9) ~~CONTRACT~~ FINAL REPORT.

(11) 1 MARCH 1976

(12) 71 p.

NRL # 528,421

(2)

(15)

CONTRACT N00014-75-C-0500
OFFICE OF NAVAL RESEARCH
DEPARTMENT OF NAVY
ARLINGTON, VA.

APPROVED FOR PUBLIC RELEASE
DISTRIBUTION UNLIMITED

RCA/GOVERNMENT AND COMMERCIAL SYSTEMS
MISSILE AND SURFACE RADAR DIVISION
MOORESTOWN, N. J.

405296

DUAL-BAND MONOPULSE ANTENNA TRACKING SYSTEM

1.0 Introduction and Program Description

For some time the Naval Research Laboratory has been investigating the usefulness of higher frequencies to improve the low-angle tracking of radar targets. The needs for long range acquisition and short range precision tracking were met with a combined and dual-mounted antenna system at X-band and at Ka-band. Tests* of these two radars with the two antennas mounted on a common pedestal proved the usefulness of the concept.

As a next step in developing a combined configuration which would be improved operationally, it was suggested that the two bands be combined into a single antenna system using only one aperture. While dual-band antennas have been used previously, the requirements for precision monopulse tracking with a common boresight at two such high frequencies made it advisable to demonstrate the technique by means of an experimental breadboard. During conversations between RCA and NRL engineering personnel, details of an antenna system were worked out in the fall of 1974.

The concept** was based upon a front fed parabola at X-band and a Cassegrain feed at Ka-band. The two feeds would be separated by a sub-reflector made in the form of a polarized grating. Thus, the two bands would use orthogonal linear polarizations. This polarization expedient was chosen because it was operationally adequate and it allowed the development of a fully dichroic sub-reflector to proceed at its own schedule.

---

* R. T. Davis, Ed. "MM Radar Tracks Low-flying Targets", Microwaves; December 1974; pp 12-14.

** RCA, MSRD "Dual-Frequency X/Ka-Band Antenna System Employing a Polarization-Selective Sub-reflector", Proposal to NRL; No. 6R3090E, 30 Sept. 1974.

The characteristics of a precision tracking radar, the AN/TPQ-27, developed by RCA for U. S. Marine Corps use were such that with minor changes the antenna and feed were applicable for such a dual-band system. The general nature of the proposed antenna evolved into this:

o	X-band feed	AN/TPQ-27 design
o	Ka-band feed	a design being used at NRL
o	Main reflector	a new procurement
o	Sub-reflector	a new design

The Ka-band feed and the main reflector were supplied as GFE* by NRL. The X-band feed was a refurbished engineering breadboard model built by RCA during the AN/TPQ-27 program. The quadrapod struts were redesigns from the same program. The polarized sub-reflector was a new design, specifically for the X/Ka system.

2.0 Description of Antenna

2.1 Antenna System

The dual frequency antenna consists of a parabolic main reflector having an aperture diameter of 8 feet and a focal length of 36 inches. Two separate feed systems are used to accommodate the two frequency bands. The X-band feed system is a five horn monopulse feed located at the focal point of the parabolic reflector. The Ka-band feed system uses a Cassegrain sub-reflector illuminated by a five horn monopulse feed. The sub-reflector consists of a parallel wire grid which is transparent to the front fed X-band feed system and acts as a highly reflective hyperbolic Cassegrain sub-reflector for the Ka-band feed system.

* Both items were built by: Ancom, Inc. (Structural Technology Div.)
1000 Ames Avenue
Milpitas, Calif.

The antenna geometry is shown in figure 2-1. The effective diameter of the hyperbolic sub-reflector is slightly under 10 inches. The sub-reflector is located so that its edge intercepts the main reflector edge ray angle of 67.34° and its image focal point is coincident with the main reflector focal point. The Ka feed horn phase center is located at the prime focus of the sub-reflector.

Figure 2-2 is a photograph of the dual frequency antenna in the test chamber showing the X-band feed-comparator with sub-reflector attached and the Ka-band feed-comparator extending from the center of the main reflector. Figure 2-3 is another photo showing more detail of the sub-reflector and support structure. The Ka-band feed comparator is enclosed in the cylinder capped with a radome which extends from the vertex of the main reflector.

2.2 X-Band feed and comparator

The X-band feed and comparator were designed for use on the AN/TPQ-27 system. The design stems from a 5-horn feed development which led to a successful incorporation into the AN/MPS-36 radar for C-band. It was scaled and improved for the AN/TPQ-27 operating at 8.5 to 9.6 GHz. The outside error horns are ridgeloaded and contiguous with the center sum-pattern horn. This latter is circular and dielectric-loaded (boron nitride) to reduce its cross-sectional diameter; the dielectric extends from the horn to create an end-fire radiator with improved sum-pattern beam shape.

The comparator is located at the feed-horn and forms a compact assembly with minimal blockage. All horns can be excited with either horizontal or vertical polarization. The four waveguide struts which support the feed assembly connect the comparator to the rear of the main reflector with both horizontal and vertical excitations for all three comparator outputs. Only one set (vertical polarization) is used.

The feed-comparator assembly is a refurbishment of an engineering breadboard model. This amounted to sealing the unit to maintain pressure, limited to 2 psi,and cleaning and painting. Because of the original experimental nature of the unit, tuning adjustments are not designed for full high power capability, particularly in the unused comparator portion, i.e., the horizontal polarization portion. It is believed, however, that the used portion, vertical polarization, will handle peak powers up to 275 kw with a 0.25 us pulse.

The X-band feed-comparator assembly with the gridded sub-reflector is supported at the focal point on a quadripod. Waveguide runs (WR 112) extending to the feed horn are utilized to form the legs of the quadripod. The general feed support arrangement is shown in Figure 2-2. The legs of the quadripod are along the 45° planes with respect to the principal planes (i.e., the vertical and horizontal), and lie at 45° with respect to the reflector axis. The quadripod connections at the reflector back structure will allow an axial adjustment of the feed-horn aperture center of ±0.25 inches.

Each leg is made up of two waveguide pieces joined at the narrow wall, each guide carrying a separate polarization. Three of the legs are active lines for the 2 pairs of polarization for the sum and 2 difference channels. The fourth leg is made identically but is inactive.

The waveguide size was changed from WR-90 to WR-112, a larger size, so that losses would be reduced. The comparator ports are in WR-90 guide size. A guide size transformer was built into each strut guide at the comparator end of the strut.

2.3 Sub-Reflector

The sub-reflector design was carried out substantially as planned and described in the RCA proposal**.

The electrical design was optimized to produce a good reflecting surface at Ka-band frequencies and at the same time be transparent to X-band frequencies of the orthogonal polarization. Several sub-reflector types were originally considered. Among those that showed the most promise were dichroic surfaces, waveguides beyond cutoff and parallel wire grids. Since the high frequency system requires a sub-reflector with a high quality precision surface, the most basic and simplest design is to be preferred both electrically and with regard to manufacturing capability. The wire grid design was selected as the lowest risk approach which results in the shortest development schedule and minimum program cost. The basis for the wire grid design is given in a paper by Mumford(1) who has derived an empirical relationship which has been reduced to nomographic form and is included here as Figure 2-4. The nomograph shows the transmission characteristics through a grid of wires for normal incidence angles with the electric vector parallel to the wires. The variables are wire diameter and center-to-center wire spacing. Figure 2-5 shows the relationship between wire radius and spacing which will limit the Ka-band leakage through the wire grid sub-reflector to a level of -15 dB down from the incident signal. Conversely, the wire grid design is required to have the opposite effect on the X-band feed, that is, to efficiently pass the X-band feed radiated power with a minimum of reflected signal. To compute the power reflection coefficient of the sub-reflector at X-band, the equation

** RCA, MSRD "Dual-Frequency X/Ka-Band Antenna System Employing a Polarization-Selective Sub-Reflector", Proposal to NRL; No. 6R3090E, 30 Sept. 1974.

derived by H. Lamb and published in a paper by Larsen[2] is given below:

$$r_p = \frac{\left[\frac{2\pi^2 a^2}{\lambda d}\right]^2}{1 + \left[\frac{2\pi^2 a^2}{\lambda d}\right]^2}$$

where: r_p is the power reflection coefficient for normal incidence and perpendicular polarization

d is the center to center wire grid spacing

a is the wire radius

λ is the free space X-band wavelength

For a wire diameter of .032" and a center to center spacing of 0.1", the reflected power at X-band will result in a sub-reflector VSWR of 1.08 which will have only a minor effect on the overall feed VSWR. The corresponding leakage power loss at the Ka-band through the sub-reflector for the Cassegrain feed will be less than 0.14 dB.

2.3.1 Power handling

As the peak powers of both the X-band and Ka-band transmitters are high, power breakdown at the sub-reflector must be considered. The question arises in the design as to the effect on the power handling capability of either bonding or not bonding the ends of the wires together. The one known reference[3] which considered these phenomena is rather unclear in data presented and in solutions to the problems. Two types of breakdown are postulated:

1 - breakdown at the wire ends for field excitation parallel to the wires, and

2 - breakdown from wire-to-wire for field excitation normal to the wires.

Experimental tests were therefore carried out to determine the relative merits of the two approaches.

A 5.4-GHz transmitter, capable of peak power outputs up to nearly one megawatt, was used in the test program. Three small-area models were constructed (see Figure 2.6); two of the samples were scaled from the X-Ka design, and the third consisted of very thin wires closely spaced and imbedded in plastic.

Each sample was tested under two conditions:

1 - the incident electric field polarized parallel to the grid wires, and

2 - polarized perpendicular to the grid wires.

No corona or breakdown was observed on any of the three samples for either polarization at field intensities of from 50,000 to nearly 100,000 volts per meter impinging on the samples. Similar results were obtained with the ends bonded together on the first two samples.

Another test was made with two equal-length, closely-spaced parallel wires one-half wavelength long for a worst case condition. Breakdown occurred at a field intensity of 47,000 volts per meter for bonded ends and perpendicular polarization.

In the referenced work, breakdown was observed for parallel polarization and unbonded ends at a field intensity of 130,000 volts per meter, and for perpendicular polarization and bonded ends at a field intensity of about 65,000 volts per meter.

The field intensities estimated for the proposed application are:

X-band (250 KW peak)	73,000 volts per meter
Ka-band (135 KW peak)	51,000 volts per meter.

Conclusions from this work were:

1 - for parallel polarization:

a - sufficient power was not available to duplicate Topper's results,

b - an adequate margin of safety exists for the Ka-band use.

2 - For perpendicular polarization:

a - both the breakdown with the half-wave model and the results of Topper's work indicate that bonding the ends of the wires together would be unsafe for X-band use.

Therefore bonding the wire ends together would be an improper solution for the proposed application.

2.3.2 Sub-reflector fabrication

The design for the size and shape of the sub-reflector was based upon the antenna geometry agreed to with NRL, as noted in section 2.1. The diameter of the electrical surface was established at 9.93 inches. Hyperbola constants of the design were:

a = 8.347"

b = 8.324"

for

$$\left(\frac{x}{a}\right)^2 - \left(\frac{y}{b}\right)^2 = 1 \quad \text{equation of hyperbola}$$

The surface was determined by a machined male mold on which a fiberglass-epoxy shell was formed. The fiberglass shell was fabricated by hand lay-up on an aluminum mandrel, then placed under a vacuum bag and cured at 300°F. The resin was EPON 828 epoxy with 10 to 13 parts-by-weight of hardener "D", plus 1% Eastman DOBP-N ultra-violet inhibitor. Ten layers

of 0.002-inch-thick type 108 glass was used. Total thickness of the fiberglass shell was between 0.018 and 0.020 inch.

Parallel grid wires were wrapped on the shell and held in place with teflon pins set into holes in the mandrel. The wires were bonded to the shell using an equal mixture of EPON 828 and Versamide V40 polyamide resin.

After the wires were bonded, a final machine cut was made on the wire surfaces to bring the contour closer to a true hyperboloid. A tool with constant radius of curvature at the cutting edge was used for this to simplify the machine coordinate calculations. Final contour was within 0.0011" RMS from the best fit hyperboloid

$$\frac{x^2}{(8.360)^2} - \frac{y^2}{(8.311)^2} = 1$$

Where

$$L_r = 20.1482$$

$$L_v = 3.4282$$

The small difference in vertex location, 0.013 inch, was accounted for during assembly and final positioning. The completed sub-reflector is shown in Figure 2-7.

2.3.3 Sub-reflector measurements

As a preliminary assessment of the interference effects of the polarized sub-reflector and its support structure, patterns of the X-band feed were taken with and without the assembly. These were taken at three frequencies, for both major feed planes, and for both sum and difference patterns. The comparator was used to excite the five-horn feed. As to be expected, there are perturbations in the patterns and, in the worse case,

these are somewhat greater than anticipated. Thus, for one pattern plane, at the low frequency end of the band, the sum pattern is modulated in amplitude about ±2 dB. The ripple frequency corresponds to the sub-reflector ring support dimensions, and the amplitude corresponds to a -13 dB multi-path signal. At other frequencies and conditions the ripple amplitude is half or less of this value.

A preliminary assessment of these ripples was made. To a first order computation this kind of ripple could cause paired minor lobes approaching 20 dB in amplitude at about ±8 degrees from boresight. A modification to the reflector edge support was developed as a paper design. The support ring was modified and moved to take it out of the X-band feed pattern without at the same time increasing blockage. It was decided, however, not to incorporate it into the final hardware unless secondary patterns determined the need.

2.4 Ka-band feed

The Ka-band feed was designed and built by Ancom, Inc. and was supplied as GFE by NRL. It consists of a five horn feed and monopulse comparator contained in a cylinder 17 inches long and 3 inches in diameter. The sum and two difference channels are brought out to waveguide flanges at the rear end of the cylinder as is also the pressure fitting.

No detailed engineering or performance data was shipped or supplied with the feed. As received, the waveguide flange interface was not in conformance with the arrangement specified by NRL and the assembly was returned to the vendor for modification. When returned it was incorporated into the antenna system without measurement or assessment by RCA.

Although no measurements were made on the feed-comparator assembly alone, some data was received from the vendor in response to an inquiry for another proposed use. These consisted of sum and difference patterns for the two principle planes, E and H. This data showed the sum patterns to be down about 14 dB at ±13 degrees interception angle of the sub-reflector. The first sidelobes are quite high, about 5-1/2 dB below the sum maximum. The sum pattern itself is about a half dB below the difference pattern maximum.

2.5 Main reflector

The main reflector was also designed and built by Ancom, Inc. and supplied as GFE by NRL. It has a 96-inch aperture and an F/D of 0.375. As received it had no bench marks, other than an axial hole, to locate the focal point. The NRL-specified surface accuracy is 0.010-inch rms.

3.0 Measurements and Test Results

Performance of the antenna was demonstrated by tests conducted per the RCA test procedure XKAD-100 Rev. A dated December 3, 1975 which is included as attachment I. The test results are tabulated in the data sheets that are included as part of the test procedure in attachment I. The antenna patterns recorded during the tests are included in attachment II.

A summary of the measured antenna performance is shown in Table 3-1 and 3-2. This table includes a column showing calculated performance based on AN/TPQ-27 antenna performance, measured X-band primary patterns with and without the sub-reflector in place, primary pattern data supplied with the ANCOM Ka-band feed, and calculated sub-reflector and strut blockage effects. In some cases, as noted in the table, the measured performance is based on measurements performed prior to the formal acceptance tests but

Table 3-1. Summary of X-Band Performance

	Measured	Calculated
Gain: (Mid-band)	43.5 dB	43.9 ±.5 dB
Beamwidth: (Nominal)		
E-Plane	.85°	.84°
H-Plane	.95°	.94°
Sum Pattern Sidelobe: (Maximum)		
E-Plane	23.5 dB	20 dB
H-Plane	22.7 dB	20 dB
Error Pattern Peak Separation: (Nominal)		
E-Plane	1.5°	1.5°
H-Plane	1.4°	1.4°
Error Pattern Null Depth: (Nominal)		
E-Plane	34 dB*	30 dB
H-Plane	34 dB*	30 dB
Error to Sum Relative Gain: (Nominal)		
E-Plane	-4.9 dB*	-5.0 dB
H-Plane	-3.7 dB*	-5.0 dB

* Values based on measurements made 11/26/75 prior to final acceptance test data.

Table 3-2. Summary of Ka-Band Performance

	Measured	Calculated
Gain: (Mid-band)	49.1 dB	52.5 dB
Beamwidth: (Nominal)		
E-Plane	.26°	.26°
H-Plane	.26°	.26°
Sum Pattern Sidelobe: (Maximum)		
E-Plane	21.0 dB	≥ 20 dB
H-Plane	20.5 dB	≥ 20 dB
Error Pattern Peak Separation: (Nominal)		
E-Plane	.35°	.35°
H-Plane	.35°	.35°
Error Pattern Null Depth: (Nominal)		
E-Plane	> 32 dB	≥ 30 dB
H-Plane	> 34 dB	≥ 30 dB
Error to Sum Relative Gain: (Nominal)		
E-Plane	+1.0 dB	-4 dB
H-Plane	-2.5 dB	-4 dB

after final antenna-feed alignment. A greater number of data samples were available during these pre-acceptance tests and it is felt the measurements are more representative of the antenna performance.

3.1 X-band results

3.1.1 Gain

The gain measured in the final acceptance test was 43.5 dB. This value is lower than a set of gain values measured prior to the formal acceptance tests but after final antenna alignments. The pre-acceptance tests gain averaged 44.5 dB. An average of the two measurements is 44 dB which compares favorably with the computed gain based on AN/TPQ-27 antenna data as shown in Table 3-3.

Table 3-3

100% Efficiency Gain	+47.5 dB
TPQ-27 feed efficiency	- 2.5 dB
Increased Blockage Losses	- 0.12 dB
Sub-reflector Losses	- 0.3 dB
Phase Distortion Losses	- 0.2 dB
Waveguide Strut Losses	- 0.25 dB
VSWR Losses	- 0.22 dB
Net Antenna Gain	+43.91 dB

3.1.2 Sidelobes

The maximum sidelobe levels generally occur for the second sidelobe. Patterns measured with and without the sub-reflector in place showed that the second sidelobe levels are increased by 2 to 4 dB with sub-reflector in place.

Since the sidelobe levels in the AN/TPQ-27 antenna at the frequencies used for the NRL antenna are generally very low (in the range of 24 to 27 dB down), the increase in level due to the effects of the sub-reflector do not cause the maximum sidelobe levels to increase above 22 dB.

3.1.3 Beamwidth

The measured beamwidths agree very closely with computation based on the AN/TPQ-27 feed characteristics. The sub-reflector had no measurable effect on the beamwidths.

3.1.4 Error pattern characteristics

The measured error pattern peak-to-peak separations agree precisely with predictions based on the TPQ-27 feed characteristics. Examination of the H-plane error-to-sum relative gain data showed that the final test data did not repeat pre-acceptance test data obtained previously. It was determined that there was an operator procedural error in obtaining the error pattern data. The test pedestal was misaligned in elevation, when measuring the error pattern by taking an azimuth cut on the test pedestal. This resulted in abnormally low error channel gain since the pattern cut was not made through the peaks of the error lobes.

Previously measured H-plane error data showed the relative gain to be 3.7 dB and the null depth to be 34 dB which agrees very closely with expected results based on AN/TPQ-27 data. Figure 3-1 shows the H-plane error and sum patterns measured on 11/26/75 which were with the proper

elevation pointing of the test pedestal.

3.2 Ka-Band Results

The sub-reflector and Ka-feed positions were initially determined using a simple rectangular aperture Ka horn since the phase center of the CFE end item Ka-band feed horn was unknown. After optimizing the sub-reflector and feed focus, measurements with the simple horn feed showed the beamwidths to be approximately 0.26° and 0.24° in the E- and H-planes respectively, with maximum sidelobe levels ranging from 16 dB to 20 dB. A rather quickly made gain measurement to determine if the gain was in the ball park of the expected value indicated a gain of 52.6 dB. This was close enough to expectations that the sub-reflector was judged to be properly positioned and functioning satisfactorily.

The ANCOM monopulse feed was then mounted and positioned for best performance. While going through the feed positioning procedure, pattern measurements indicated very low sum channel gain relative to the error channel gain. The horn was removed from the antenna for visual examination and VSWR measurements.

Not much could be determined by visual inspection. VSWR measurements repeated very closely data submitted by ANCOM with the feed horn and do not account for the low sum channel gain. It is felt that there may be internal losses within the feed, possibly related to the coupler in which a portion of the sum channel energy is coupled into the four error horns.

The horn was remounted in the antenna and pattern testing continued with no further explanation of the low sum channel gain.

3.2.1 Gain

The gain measured in the final acceptance test was 49.1 dB which repeated the results of pre-acceptance test measurements. The predicted antenna gain for the Ka-band feed system is 52.5 dB. Table 3-4 shows the factors considered in predicting the Ka gain. Feed horn pattern data submitted by ANCOM were used to calculate the feed spillover losses and aperture taper efficiency.

The measured gain of the error peaks at midband, 50.2 dB and 48.2 dB for the E- and H-plane error channels, are reasonable based on the predicted sum channel gain of 52.5 dB. Which indicates that the low sum channel gain is probably due to excessive losses in the feed horn sum channel and not caused by the main reflector or sub-reflector.

Table 3-4

Ka-Band Antenna Gain

100% Efficiency Aperture Gain	+59	dB
Feed Spillover Losses	- 3.5	
Aperture Taper Efficiency	- 0.7	
Aperture Blockage Losses	- 0.4	
Surface Tolerance Losses	- 1.3	
VSWR Losses	- 0.2	
Estimated Feed Losses	- 0.4	
Net Antenna Gain	+52.5	dB

3.2.2 Sidelobe levels

The maximum sidelobe levels measured between 20.5 dB and 23 dB. The final feed/sub-reflector position was based on a tradeoff between E- and H-plane depth of nulls between the main beam and first sidelobe and the first sidelobe levels. No feed/sub-reflector position was found that would produce deep nulls for both E- and H-plane patterns. A compromise position was selected where the E- and H-plane pattern characteristics are similar. Final positioning of the Ka-feed and pinning of the sub-reflector resulted in a slight asymmetry in the E-plane (azimuth plane of antenna) pattern sidelobe characteristics.

3.2.3 Beamwidth

The half power beamwidths measured were between 0.25° and 0.27° with most of the measurements right on the expected beamwidth of 0.26°.

3.2.4 Error pattern characteristics

The measured error pattern peak-to-peak separation angle 0.35° agrees with predicted performance based on primary error pattern data submitted by ANCOM. The primary error pattern data showed a 13° peak-to-peak separation which is equivalent to a 1.5 inch error horn spacing. In the Cassegrain antenna geometry, which has an equivalent focal length of 210.65 inches, the theoretical error pattern for horns spaced 1.5 inches has a peak-to-peak error beam separation of 0.35°.

The error pattern null depths were observed to vary considerably in the orthogonal plane, i.e., an elevation error pattern null level varied greatly in the azimuth plane at the elevation null angle. Thus when measuring the elevation error pattern, the apparent null depth would vary considerably depending upon alignment of the azimuth angle. This effect

was greatest for the elevation error channel at 35 GHz. A measured null depth of 30 dB relative to error was obtained with the test pedestal fixed at a 2.31° elevation angle (the pattern measurement was made by rotating the test pedestal in azimuth with the antenna rotated 90° about its polarization axis so the antenna elevation axis is coincident to the test pedestal azimuth axis). With the test pedestal aligned in elevation for maximum Ka error lobe peaks, the pedestal elevation axis was 2.42° and the measured null depth relative to error peak was only about 10 dB. This null fillin is not due solely to pre-comparator phase error, since, if it were the null level in the orthogonal axis would have the shape of a sum lobe and drop off less than 3 dB between the 2.31° and 2.42° angle.

It is possible that there is some error channel and/or sum channel cross coupling due to the coupling network within the feed that is contributing to this effect.

3.3 X-Band/Ka-Band Beam Alignment

The error pattern null positions were used as the beam pointing angle reference. The X-band beam position is determined primarily by the position of the X-band feed relative to the focal axis of the reflector. During assembly of the X-band feed/comparator to the reflector a precise mechanical alignment procedure was followed to insure accurate positioning of the feed with respect to the reflector focal point. X-band pattern measurements verified proper feed position.

The Ka-band beam position is determined primarily by the position of the hyperbolic sub-reflector foci and secondarily by the Ka-band feed position. The sub-reflector is supported by an adjustable bracket from the X-band feed/comparator to permit it to be adjusted independently of the X-band feed.

During initial sub-reflector position optimization with the single horn Ka feed, the effect of sub-reflector translation on Ka to X-band beam position was measured. The sub-reflector was offset 1/8 inch to the left of the nominal center position. The center of the Ka beam shifted approximately 2.3 milliradians to the right of the X-band error pattern null. This agrees very closely with the theoretical Ka-beam shift of 2 milliradians per 0.1-inch sub-reflector offset. The best collimation of the X/Ka beams was obtained with the sub-reflector at its center position established during initial mechanical alignment of the feed/sub-reflector support bracketry. No readjustment of the sub-reflector offset for beam collimation was required after the single horn Ka feed was replaced with the final ANCOM Ka feed.

4.0 Conclusions

1 - The test results show there are no excessive losses or pattern degradation due to the sub-reflector at either X- or Ka-band, verifying the feasibility of the dual frequency antenna with the parallel wire grid sub-reflector.

2 - The dual frequency configuration has reduced the X-band performance as predicted. The predicted 1/2 dB gain loss at X-band was due to 0.3 dB reflection losses of the dielectric sub-reflector and phase and amplitude ripple introduced to the primary pattern which contributed 0.2 dB to the loss and had a minor effect on the sidelobe levels. These losses could be reduced by improved sub-reflector design to minimize X-band scattering.

3 - The Ka-band difference channel pattern peak gain measured within expected values verifying good antenna performance at Ka-band.

4 - The Ka-band feed appears to have excessive loss in the sum channel.

5 - The Ka-band feed may have excessive cross coupling between sum and difference channels which could explain difference channel null depth problems evidenced at the high end of the Ka-band.

References:

(1) Mumford, W. W., "Some Technical Aspects of Microwave Radiation Hazards", Proc. IRE Vol. 49, p. 444-5, Feb. 1961.

(2) Larsen, T., "A Survey of the Theory of Wire Grids"; PGMTT; May, 1962.

(3) Topper, L., "Characteristics of Gratings and Design Techniques at High RF Power Levels"; Microwave Journal; August, 1966, p 105.

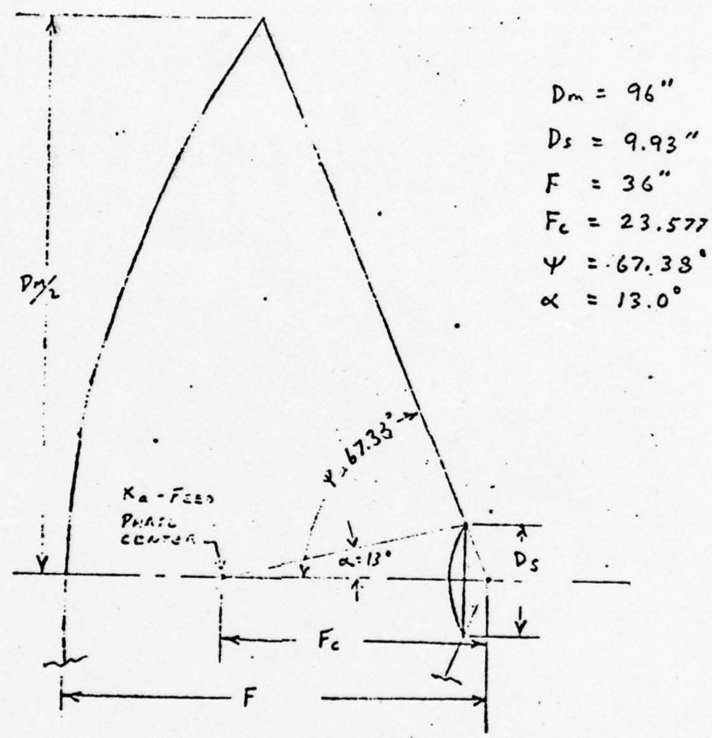

ANTENNA GEOMETRY

FIG. 2.1

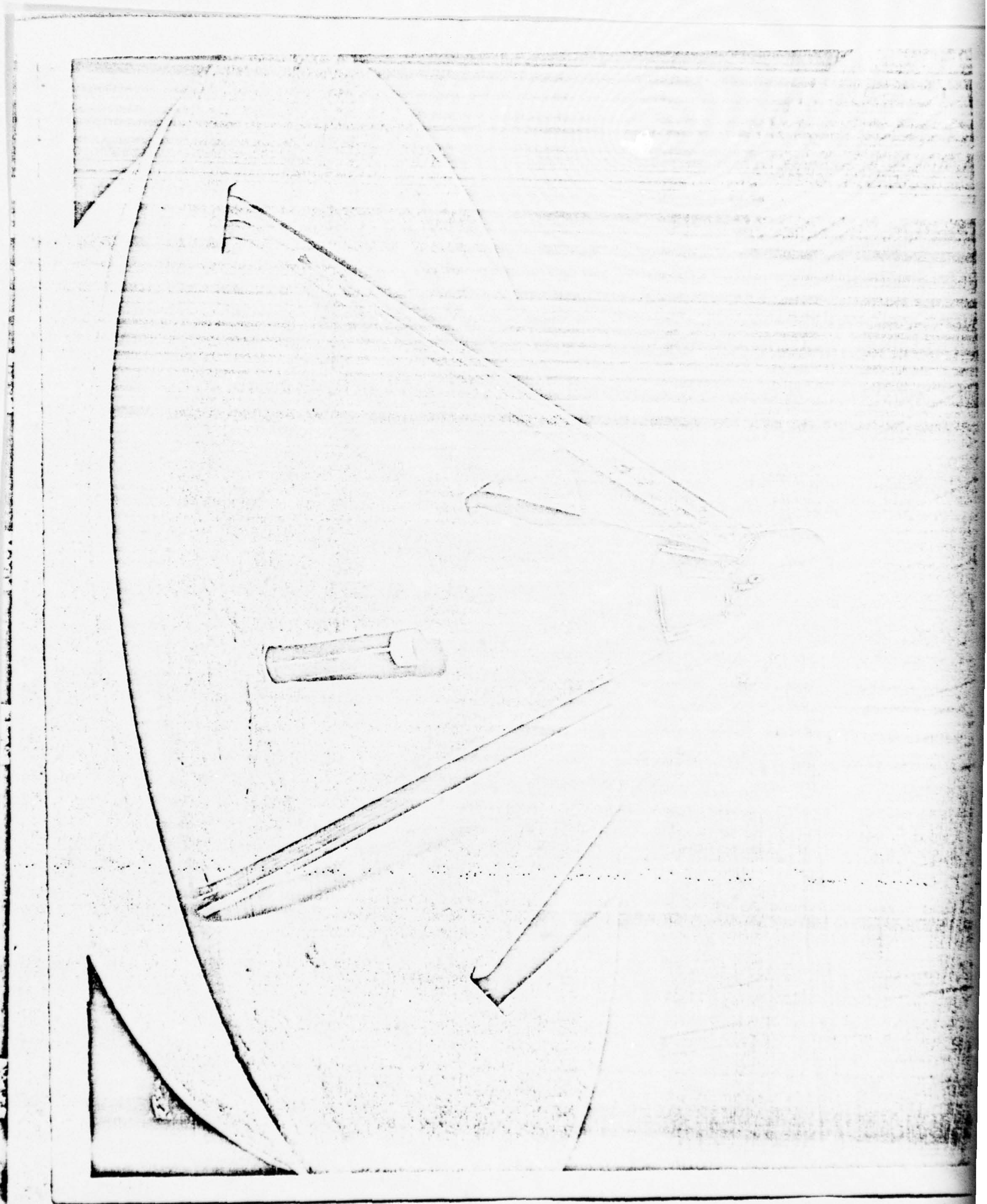

FIG 2-2 ASSEMBLED ANTENNA

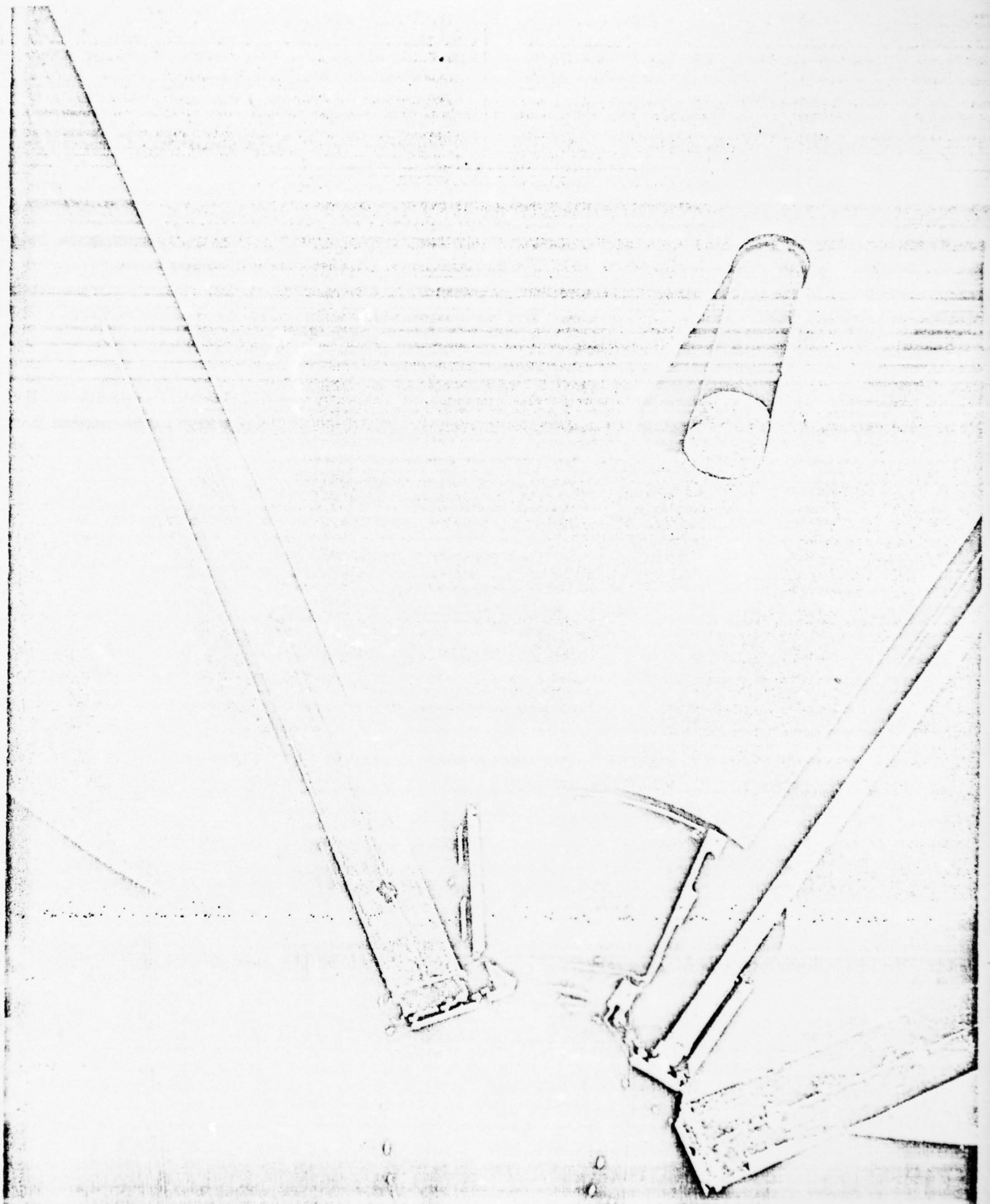

FIG 2-3 CLOSE-UP OF FEEDS

TRANSMISSION THROUGH A GRID OF WIRES

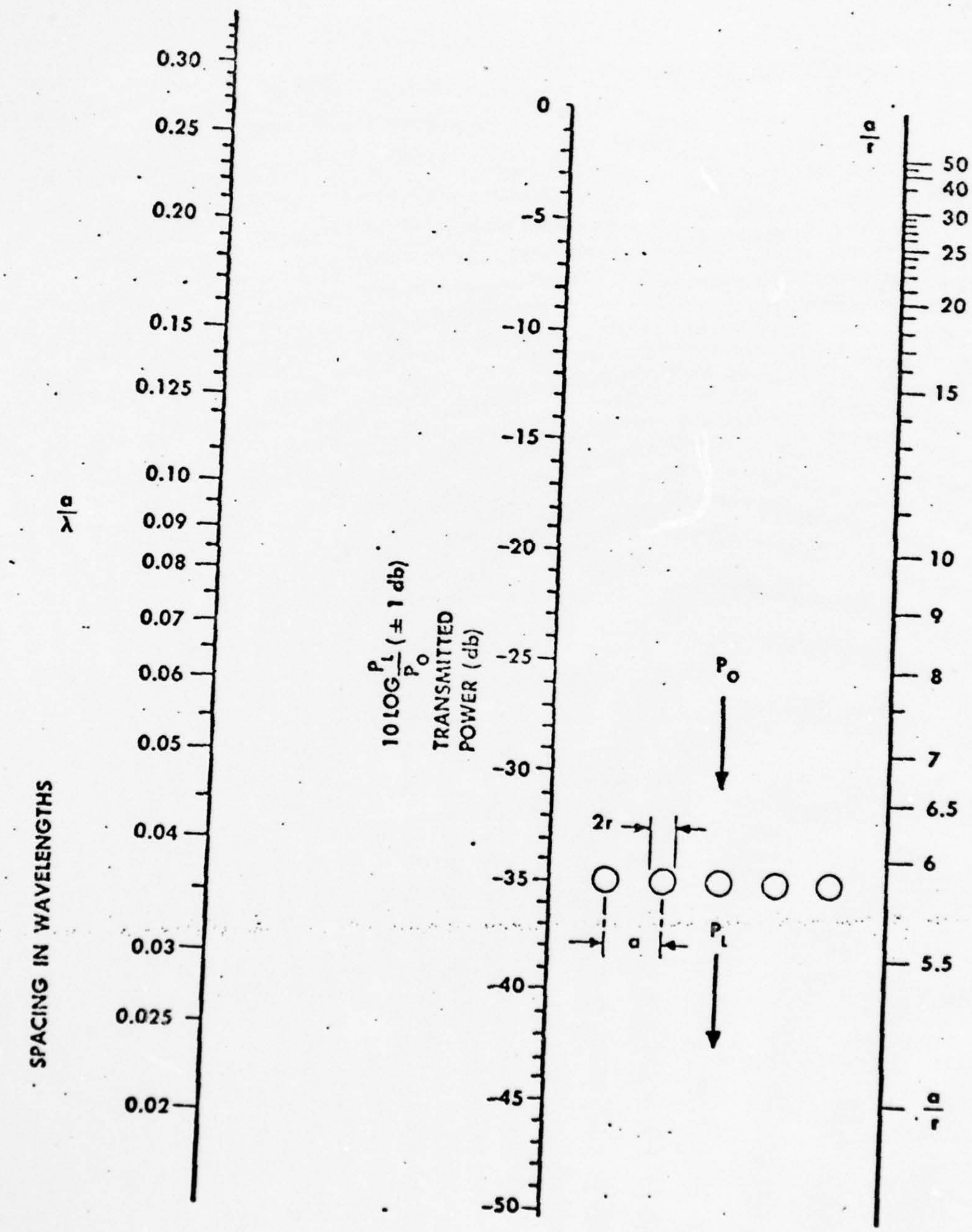

FIG. 2-4

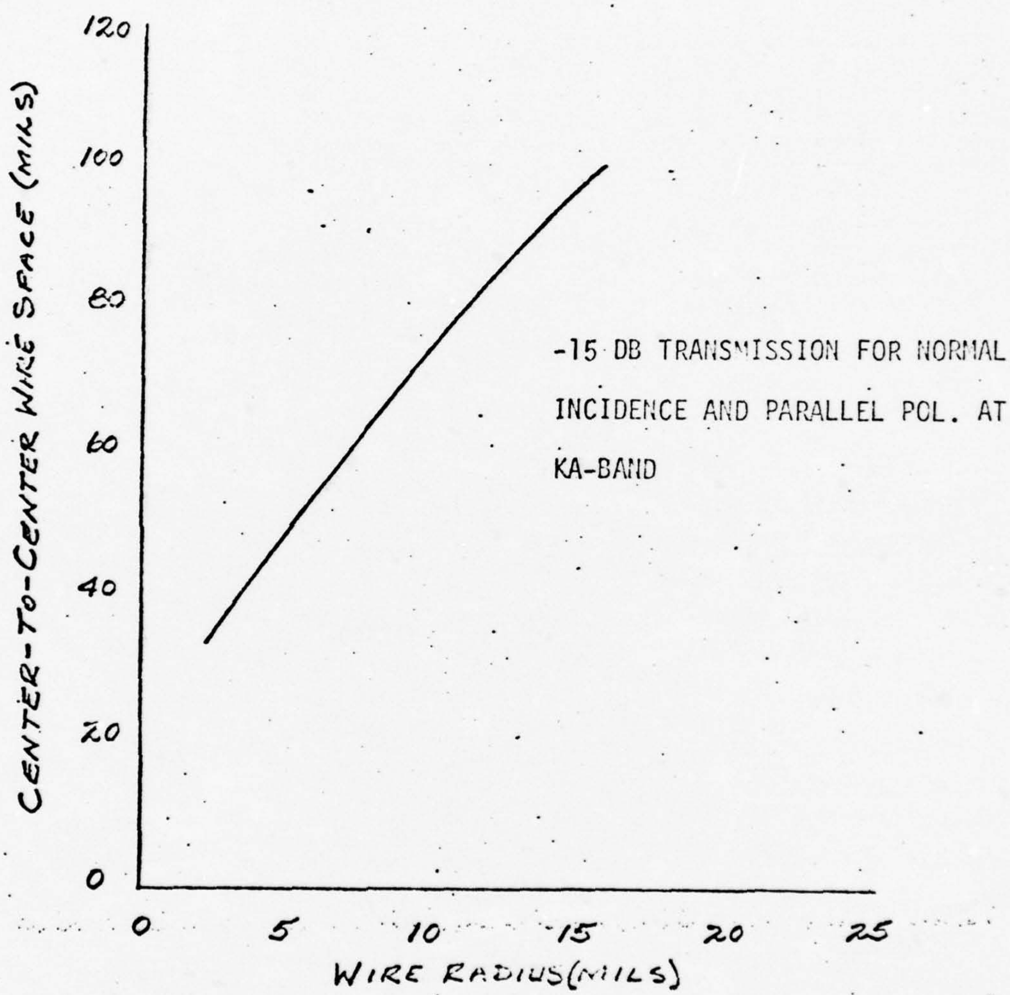

FIGURE 2-5. WIRE GRID SUB-REFLECTOR DESIGN

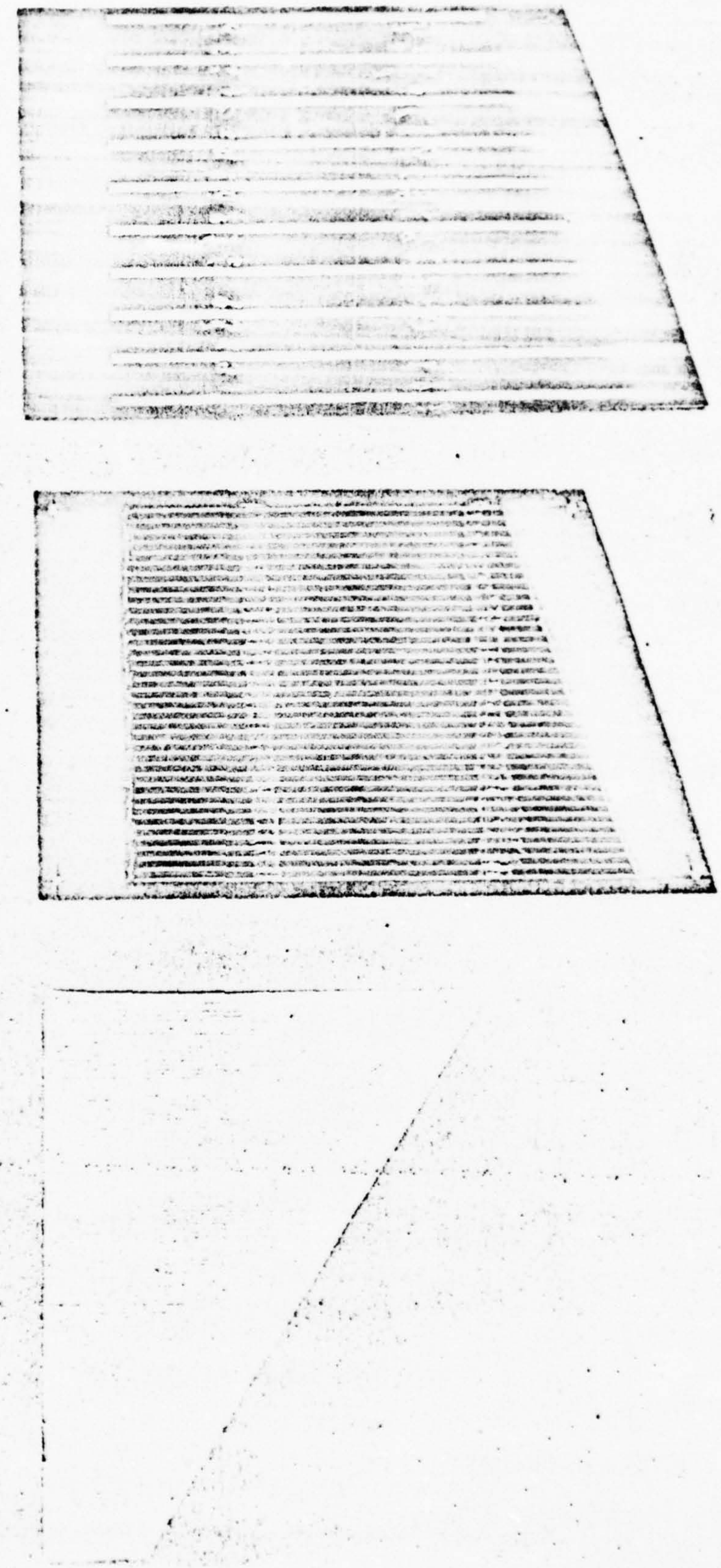

FIG 2-6 POWER BREAKDOWN - TEST GRIDS

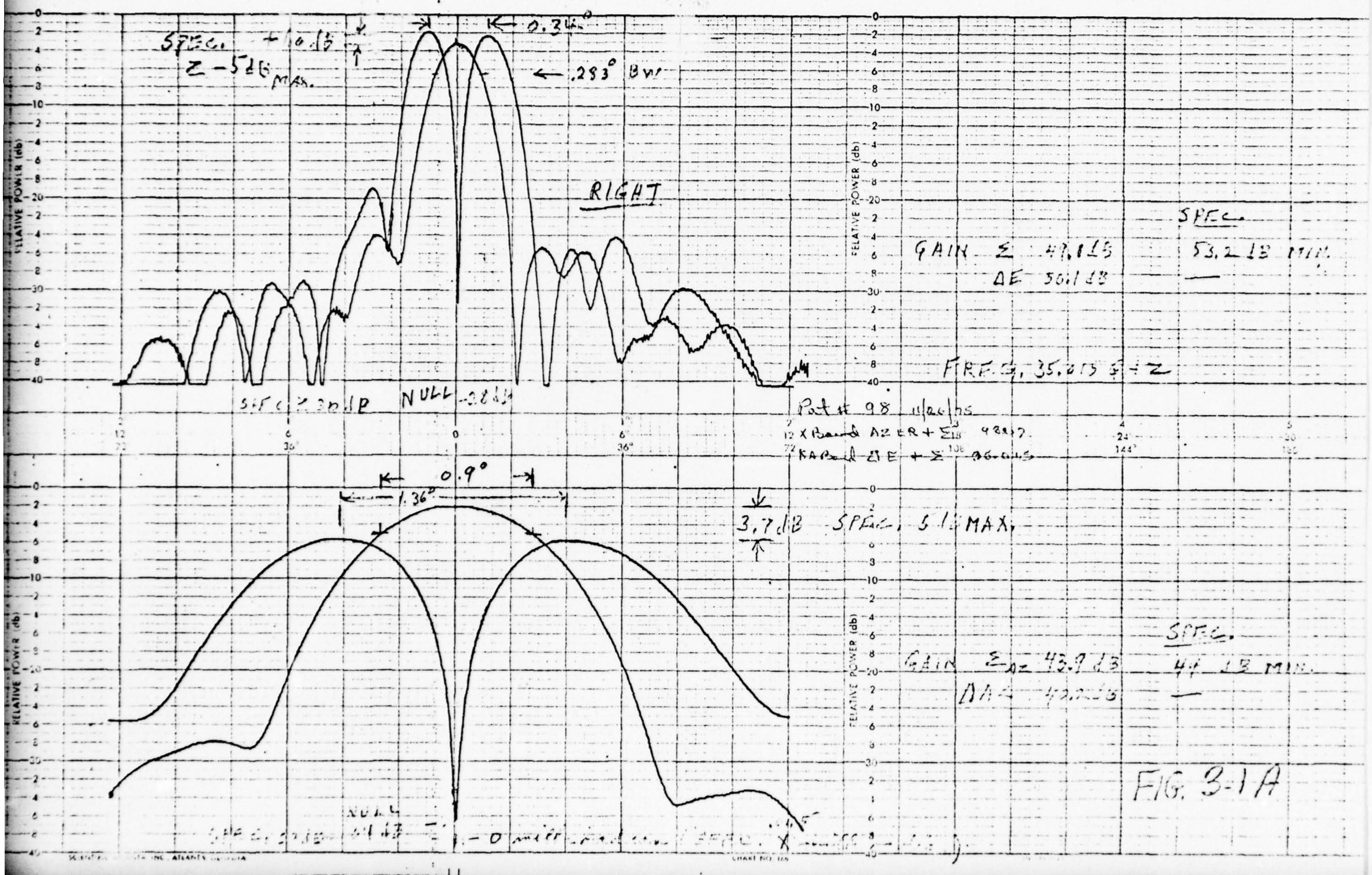
SPEC. +1 dB
Σ -5 dB MAX.
0.34°
.283° BW
RIGHT
NULL -38 dB
Part # 98 Weeks
X Band AZ ER + Σ
KA Band ΔE + Σ
0.9°
1.36°
3.7 dB SPEC. 5 dB MAX.
GAIN Σ 47.1 dB
ΔE 50.1 dB
SPEC.
53.2 dB MIN.
FREQ. 35.0 GHZ
SPEC.
44 dB MIN.
NULL
RELATIVE POWER (db)

FIG. 3-1A

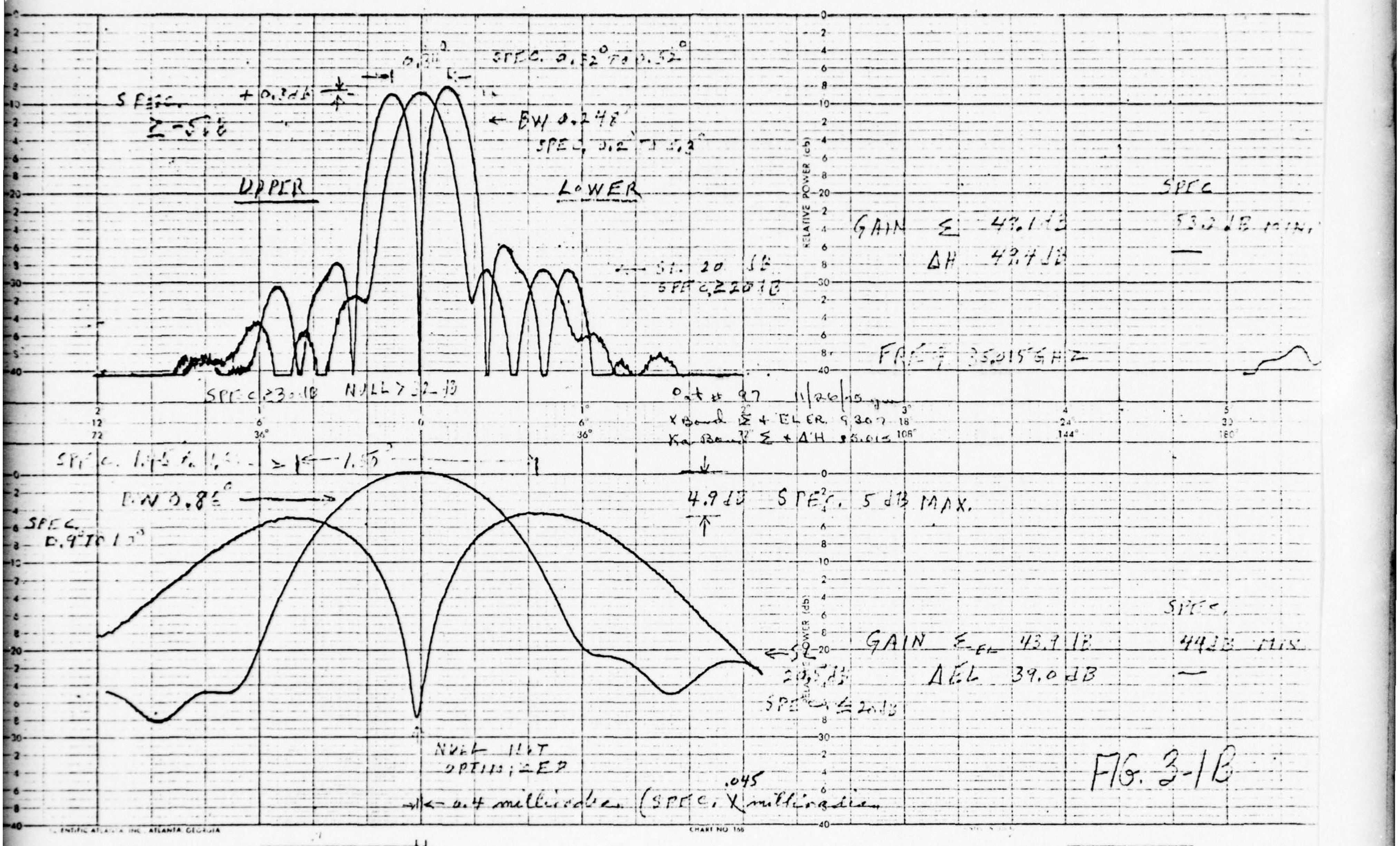

SPEC. 0.52° TO 0.52°
SPEC. Σ -5 dB
+0.3 dB
← BW 0.24°
SPEC. 0.2° TO 0.3°
UPPER
LOWER
SL 20 dB
SPEC ≥ 20 dB
SPEC ≥ 23 dB
NULL > 32 dB
GAIN Σ 43.1 dB
ΔH 42.4 dB
SPEC
53.0 dB MIN.
FREQ 35.015 GHZ
X Band Σ + ΔEL 9.307
Ka Band Σ + ΔH 35.015
SPEC. 1.4° TO 1.6°
1.55°
BW 0.85°
SPEC. 0.9° TO 1.3°
4.9 dB SPEC. 5 dB MAX.
GAIN Σ EL 43.9 dB
ΔEL 39.0 dB
SPEC.
44 dB MIN.
SL 20.5 dB
SPEC ≥ 20 dB
NULL NOT OPTIMIZED
0.4 milliradian (SPEC. .045 X milliradian
RELATIVE POWER (db)
CHART NO 166

FIG. 3-1B

XKAD-100
June 17, 1975
Rev. A, December 3, 1975

TEST PROCEDURE

FOR

DUAL-FREQUENCY X/Ka-BAND ANTENNA SYSTEM

PREPARED FOR:

NAVAL RESEARCH LABORATORY
Washington, D. C.

PREPARED BY:

RCA/Government and Commercial Systems
Missile and Surface Radar Division
Moorestown, New Jersey

APPROVED BY:

W C Wilkinson RCA ENG.

R. L. Hinks RCA PMO

J Mclugh 12/10/75 NRL

TEST PLAN FOR NRL DUAL FREQUENCY X/Ka-BAND ANTENNA

1.0 PURPOSE OF TESTS

The purpose of the tests described in this document is to demonstrate the performance of the 8 foot diameter dual frequency X/Ka-band antenna. The antenna consists of a customer furnished 8 foot diameter paraboloid reflector and Ka-band monopulse feedhorn and comparator and RCA furnished X-band monopulse feedhorn and comparator, a polarization selective hyperboloid sub-reflector and X-band waveguide quadripod support for the X-band feed and sub-reflector. Principal plane secondary patterns are measured for both the Ka-band cassegrain antenna configuration and the X-band front fed antenna configuration. Also X and Ka-band beam collimation is measured by superimposing the appropriate monopulse error patterns.

2.0 TEST NOTES

2.1 Any deviation from these test requirements, including additional tests, are permissible only by mutual agreement between RCA and NRL.

2.2 RCA reserves the option to run tests in a sequence suited to meet total program requirements and not necessarily in numerical order.

2.3 RCA shall provide verification that test equipment used for these tests has been calibrated within acceptable time limits.

2.4 The test limits will be established by mutual agreement between RCA and NRL, after test data has been measured.

2.5 The following test equipment or equivalent is recommended for conducting the performance tests:

Attenuator	HP X382A And HPR382A
Directional Coupler	HP X752C Or E
Frequency Meter	HP X532B And HPR532A
Standard Gain Horn	NARDA 640 And TRG A890
Receiver	S. A. 1752
Pattern Recorder	S. A. 1540
Antenna Positioner	S. A. 5515C-7R
Positioner Control	S. A. 4116
Position Indicator	S. A. 4423
Field Probe Carriage	S. A. 5951
Signal Source, X-Band	S. A. 2120
Signal Source, Ka-Band	Varian VA97
VSWR Indicator	HP 415B

3.0 TEST DESCRIPTION

3.1 Secondary Pattern Test

3.1.1 Receiver Calibration

The receiver chart amplitude shall be calibrated using a calibrated variable attenuator as shown in Figure 3-1.

1. Connect the X-Band sum vertical part to one receiver.
2. Set the transmitter and receiver frequency to 9300 MHz.
3. Position antenna in azimuth and elevation for maximum signal with the calibrated attenuator set to zero dB and the pad attenuator set approximately 10 dB.
4. Set receiver gain to the 0dB calibration mark on the recorder chart and mark zero dB. Record receiver and recorder gain settings on chart.

5. Set the calibrated attenuator to 3, 5, 20, 35, and 40 dB in order and mark attenuation values on chart.
6. Reset calibrated attenuator to zero dB and note that receive signal level returns to zero dB on chart. Adjust pad attenuator to obtain 6 dB receive signal reference level on chart. Mark chart and lock pad attenuator.
7. Connect the KA-band sum horizontal port to the other receiver.
8. Set the transmitter and receiver frequency to 34.86 GHz.
9. Repeat steps 3-6.

3.1.2 X-Band Reference Patterns

The beamwidth and sidelobe levels of the X-band transmit/reference channel shall be measured at three frequencies, 9050 MHz, 9300 MHz and 9550 MHz using the following procedure and equipment set up shown in Figure 3-1.

1. Connect the sum vertical port to the receiver.
2. Set the transmitter and receiver frequency to 9050 MHz.
3. Position antenna in azimuth and elevation for maximum signal.
4. Set the pattern recorder scale for zero degrees.
5. Record pattern in azimuth plane for approximately ± 20 degrees from boresight.
6. Repeat setps 4-5 for 9300 MHz and 9550 MHz.
7. Rotate test antenna 90° about its polarization axis, and repeat steps 3-6.
8. Record 3 dB beamwidth and maximum sidelobe levels on Data Sheet 3-1.

3.1.3 XBand Error Patterns

The null depth, peak to peak separation of the error lobes, and the error pattern gain relative to the sum pattern peak shall be measured for vertical polarization of the X-band azimuth and elevation error channels at 9050 MHz, 9300 MHz and 9550 MHz using the following procedure:

1. Set frequency to 9050 MHz.
2. Record the peak of the sum pattern over an angle ± 2 degrees from boresight as described in paragraph 3.1.2. Maintain all equipment gain settings until completion of error pattern.
3. Connect azimuth vertical port to receiver.
4. Record error pattern for an angle of approximately $\pm$ 20 degrees from boresight.
5. Repeat steps 2-4 for frequencies of 9300 MHz and 9550 MHz.
6. Rotate the test antenna 90° about its polarization axis.
7. Set the frequency to 9050 MHz and repeat steps 2-5 for the sum and elevation vertical ports.
8. Record null depth, peak to peak separation, and relative gain on Data Sheet 3-2.

3.1.4 X-Band Gain

The on axis gain of the transmit/reference channel shall be measured at the output waveguide port of the antenna assembly. The gain is measured at 9300 MHz for vertical polarization using the setup of Figure 3-1 and the following procedure:

1. Connect receiver on vertical transmit/reference port where gain is to be measured and place loads on all other ports.
2. Position the antenna in azimuth and elevation for maximum signal.
3. Adjust receiver gain for a convenient level on the recorder chart.
4. Record the peak of the sum pattern over an azimuth cut of approximately $\pm 2^{o}$.
5. Rotate pedestal 180 degrees and connect receiver to the standard gain horn.
6. Sweep the standard gain horn vertically using the field probe mechanism and record signal level on the same pattern recorder chart obtained in step 4. Maintain all equipment gain setting while making the measurement.
7. The average value of the field pattern is utilized to yield the gain of the antenna.

8. Record calibrated value of difference between antenna pattern peak and average value of field pattern on Data Sheet 3-3.

3.1.5 Ka-Band Reference Patterns

The beamwidth and sidelobe levels of the Ka-band transmit/reference channel shall be measured at 34.86 GHz using the following procedure and equipment set-up shown in Figure 3-1.

1. Connect the sum horizontal port to the receiver.
2. Set the transmitter and receiver frequency to 34.86 GHz.
3. Position antenna in azimuth and elevation for maximum signal.
4. Set the pattern recorder scale for zero degrees.
5. Record pattern in azimuth plane for approximately 5 degrees from boresight.
6. Rotate test antenna 90° about its polarization axis, and repeat steps 3-5.
7. Record 3 dB beamwidth and maximum sidelobe levels on Data Sheet 3-4.

3.1.6 Ka-Band Error Patterns

The null depth, peak to peak separation of the error lobes, and the error pattern gain relative to the sum pattern peak shall be measured for horizontal polarization of the Ka-Band azimuth and elevation error channels at 34.86 GHz using the following procedure:

1. Set frequency to 34.86 GHz
2. Record the peak of the sum pattern over an angle + 2 degrees from boresight as described in paragrpah 3.1.2. Maintain all equipment gain settings until completion of error pattern.
3. Connect azimuth horizontal port to receiver.
4. Record error pattern for an angle of approximately ±5 degrees from boresight.
5. Rotate the antenna 90° about its polarization axis.
6. Repeat steps 2-4 for the sum and elevation horizontal ports.
7. Record null depth, peak to peak separation and relative gain on Data Sheet 3-5.

3.1.7 Ka-Band Gain

The on axis gain of the transmit/reference channel shall be measured at the output waveguide port of the antenna assembly. The gain is measured at 34.86 GHz for horizontal polarization using the setup of Figure 3-1 and the following procedure:

1. Connect receiver on horizontal transmit/reference port where gain is to be measured and place loads on all other ports.
2. Position the antenna in azimuth and elevation for maximum signal.
3. Adjust receiver gain for a convenient level on the recorder chart.
4. Record the peak of the sum pattern over an azimuth cut of approximately $\pm 2^{o}$.
5. Rotate pedestal 180 degrees and connect receiver to the standard gain horn.
6. Sweep the standard gain horn vertically using the field probe mechanism and record signal level on the same pattern recorder chart obtained in step 4. Maintain all equipment gain setting while making the measurement.
7. The average value of the field pattern is utilized to yield the gain of the antenna.
8. Record calibrated value of difference between antenna pattern peak and average value of field pattern on Data Sheet 3-3.

3.1.8 X/Ka-Band Beam Collimation

Collimation of the X and Ka-band beams shall be demonstrated by super position of the appropriate X-band and Ka-band monopulse error patterns on the same pattern recorder chart using the following procedure:

1. Set the X-band frequency to 9300 MHZ
2. Set the Ka-band frequency to 34.86 GHZ
3. Connect the azimuth vertical X-band port to the receiver.
4. Record the X-band error pattern for an angle of approximately $\pm 2^{o}$ using the expanded ($\pm 5^{o}$) angle scale.

5. Without readjustment to the pattern recorder angle axis, connect the azimuth horizontal Ka-band port to the receiver.

6. Record the Ka-band error pattern for an angle of approximately + 2^o on the same recorder chart as the previously recorded X-band pattern. The signal level gain for each pattern should be set to insure that both the X-band and Ka-band nulls appear on the recorder chart.

7. Record the angular displacement between the X-band and Ka-band error nulls in Data Sheet 3-6.

8. Rotate the test antenna 90^o about its polarization axis

9. Repeat steps 3 through 7.

10. Repeat steps 1 through 9 for X-band frequencies of 9050MHZ and 9550 MHZ.

11. Repeat steps 1 through 9 for KA-band frequencies of 34.50 and 35.00 GHz with X-band frequency set to 9300 MHz.

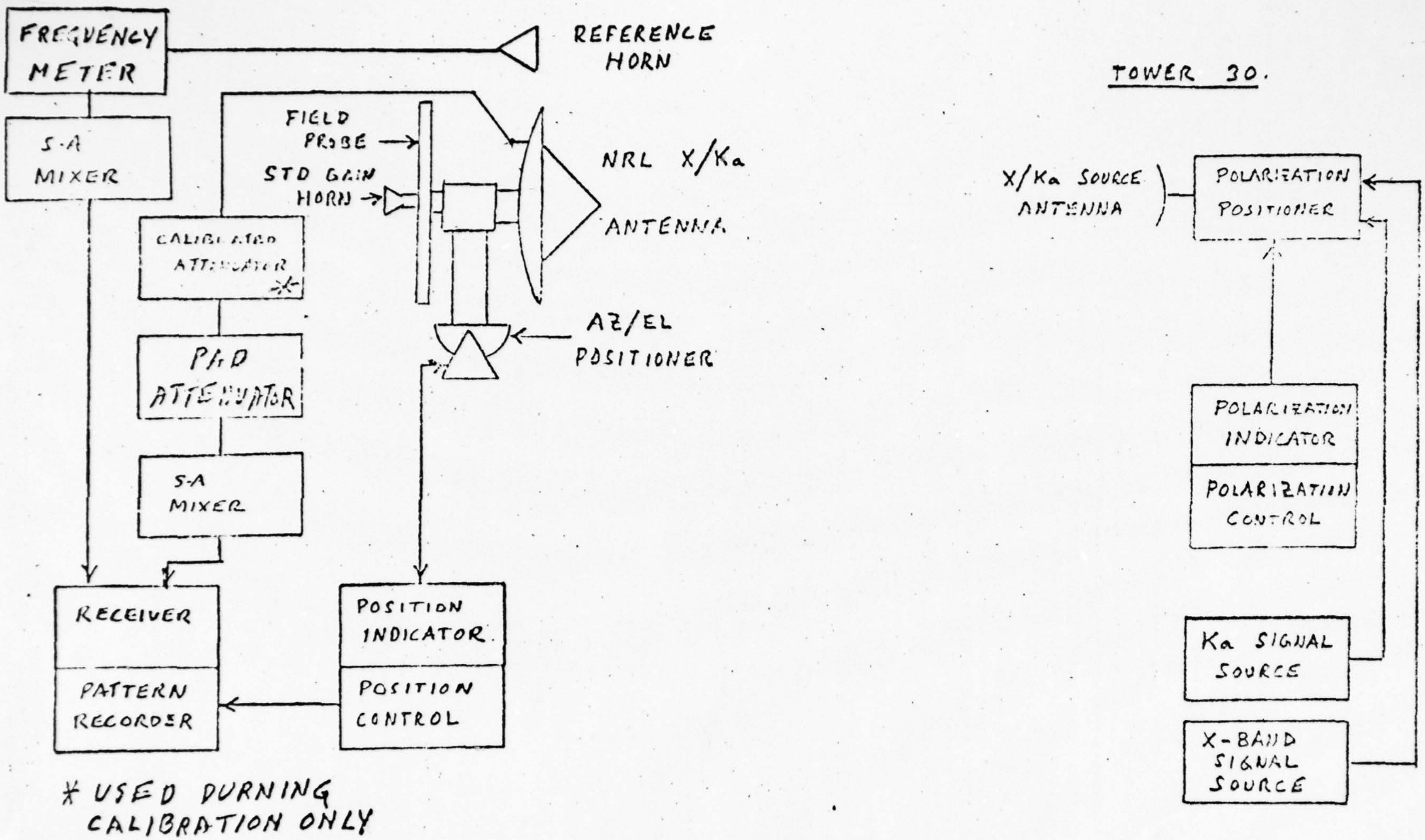

NRL X/Ka DUAL FREQUENCY ANTENNA

PATTERN TEST RANGE

FIG 3-1

DATA SHEET 3-1
BEAMWIDTH AND SIDELOBES

CHANNEL	PLANE	FREQUENCY	BEAMWIDTH	MAXIMUM SIDELOBE	No.	Date
Reference	H (Az)	9050 MHz	0.9°	22.7 dB	13	12/11/75
		9300 MHz	1.0°	23.5 dB	8	12/10/75
		9550 MHz	0.9°	23.5 dB	14	12/11/75
Reference	E (El)	9050 MHz	0.9°	26.0 dB	19	12/11/75
		9300 MHz	0.83°	26.5 dB	9	12/10/75
		9550 MHz	0.83°	23.5 dB	17	12/11/75
Test Limit (See Note 2.4)			.9° ±.1°	22.0 db		

Witness Representing: Signature Date

RCA Engineering: C. F. Crawford 12-11-75

Government: [illegible] 12/12/75

DATA SHEET 3-2
ERROR PATTERN CHARACTERISTICS

CHANNEL	PLANE	FREQUENCY	NULL DEPTH	P-P SEPARATION	RELATIVE GAIN	Pattern No	Pattern Date
Az Vert.	H	9050 MHz	37 dB	1.4°	- 4.5 dB	13	12/10/75
		9300 MHz	35 dB	1.4°	- 7.0 dB	8	12/10/75
		9550 MHz	37 dB	1.4°	- 8.0 dB	14	12/11/75
El Vert.	E	9050 MHz	39+ dB	1.[illegible]°	- 4.0 dB	19	12/11/75
		9300 MHz	38+ dB	1.5°	- 3.2 dB	[illegible]	12/10/75
		9550 MHz	38[illegible] dB	1.5°	- 4.5 dB	17	12/11/7[illegible]
Test Limit (See Note 2.4)			35 db	1.5° ± .1°	X		

Witness Representing:	Signature	Date
RCA Engineering	C. F. Crawford	12-11-75
Government	[illegible signature]	12-12-75

DATA SHEET 3-3
ANTENNA GAIN

	FREQUENCY	A GAIN OF STD HORN	B ANTENNA PEAK RELATIVE TO STD HORN	C GAIN (A&B)	LIMIT See Note 2.4	Pattern No.	Pattern Date
Σ AZ	9300	22.0 dB	21.1 dB	43.1 dB		4	12/10/75
Σ EL	9300 MHz	22.0 dB	21.8 dB	43.8 dB		5	11
Σ EL	34.86 GHz	24.6 dB	23.7+0.1=23.8 dB	48.4 dB		5	11
Σ AZ	11	24.6 dB	24.6+0.1=24.7 dB	49.7 dB		4	11

Witness Representing:	Signature	Date
RCA Engineering	C. F. Crawford	12-11-75
Government	[illegible]	12-12-75

DATA SHEET 3-4
BEAMWIDTH AND SIDELOBES

CHANNEL	PLANE	FREQUENCY	BEAMWIDTH	MAXIMUM SIDELOBE	Pattern No.	Date
Reference	H (EL)	34.86 GHz	0.25°	22.0 dB	5	12/10/75
	E (Az)	34.86 GHz	0.32°	20.5 dB	4	12/10/75
Test Limit (See Note 2.4)			X	X		
REF.	H (EL)	35.0 GHz	0.26°	23.0 dB	24	12-11-75
	E (Az)	"	0.26°	23.0 dB	23	12-11-75
	H (EL)	34.5 GHz	0.26°	21.0 dB	21	12-11-75
	E (Az)	"	0.28°	20.5 dB	22	12-11-75

Witness Representing:	Signature	Date
RCA Engineering	C. J. Crawford	12-11-75
Government	[illegible signature]	12-12-75

DATA SHEET 3-5
ERROR PATTERN CHARACTERISTICS

CHANNEL	PLANE	FREQUENCY	NULL DEPTH	P-P SEPARATION	RELATIVE GAIN	Patt. No.	Date
Az	E	34.86 GHz	32 dB	0.36°	+ 0.5 dB	7	12/9/75
El	H	34.86 GHz	34+ dB	0.36°	- 0.2 dB	6	12/9/75
Test Limit (See Note 2.4)							
AZ	E	35.00 GHz	33+ dB	0.34°	+ 1.5 dB	23	12-11-75
EL	H	"	34 dB	0.34°	-3.5 dB	24	12-11-75
AZ	E	34.53 GHz	40+ dB	0.34°	+ 0.5 dB	22	12-11-75
EL	H	"	37+ dB	0.36°	- 2.5 dB	21	12-11-75

Witness Representing	Signature	Date
RCA Engineering	C. F. Crawford	12-11-75
Government	[illegible]	12-12-75

DATA SHEET 3-6
BEAM COLLIMATION

AXIS	FREQUENCY X-Band	FREQUENCY Ka-Band	MILLIRADIAN ANGULAR DISPLACEMENT BETWEEN ERROR NULLS	Pattern No.	Pattern Date
AZIMUTH	9300 MHZ	34.50	0.4 LEFT	22	12-11-75
		34.86 GHZ	0.1 RIGHT	11	12-10-75
		35.00	[illegible]	23	12-11-75
"	9050	34.86	0.3 "	12	12-11-75
"	9550	34.86	0.3 LEFT	15	12-11-75
ELEVATION	9300	34.50	0.[illegible] DOWN	20	12-11-75
		34.86	1.0 UP	10	12-10-75
		35.00			
"	9050	34.86	0.[illegible] UP	18	12-11-75
"	9550	34.86	0	16	12-11-75
TEST LIMIT (See Note 2.4)			X		
AZ	9300 MHz	35.00 GHZ	0.4 LEFT	23	12-11-75
EL	9300 MHz	35.00 GHZ	0	24	12-11-75

Witness Representing	Signature	Date
RCA Engineering	C. F. Crawford	12-11-75
Government	[illegible signature]	12/12/75

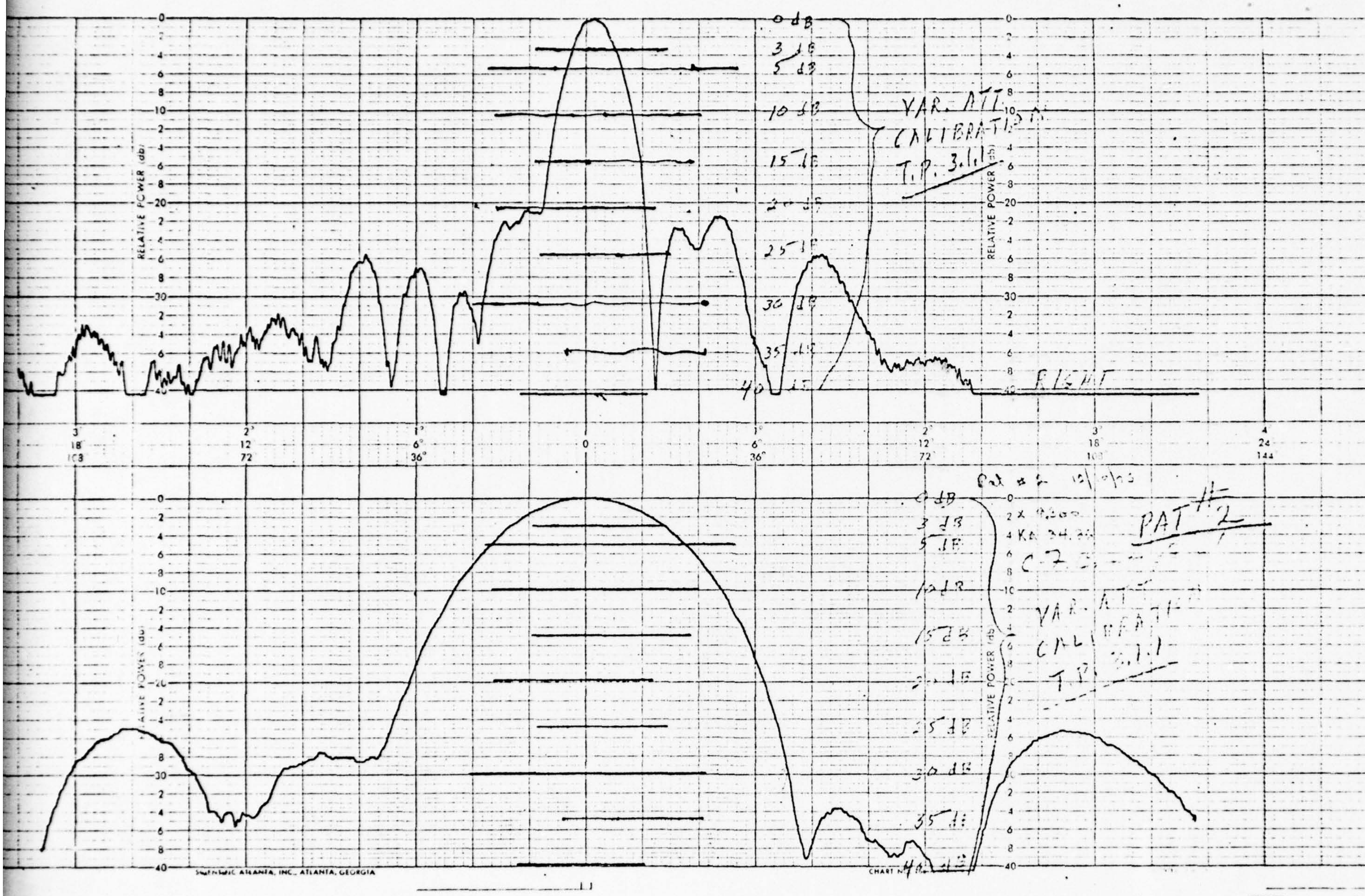
RELATIVE POWER (db)
0 dB
3 dB
5 dB
10 dB
15 dB
25 dB
30 dB
35 dB
40 dB
VAR. ATT. CALIBRATION
T.P. 3.1.1
RIGHT
PAT #2
VAR. ATT. CALIBRATION
T.P. 3.1.1
SCIENTIFIC ATLANTA, INC., ATLANTA, GEORGIA
CHART NO.

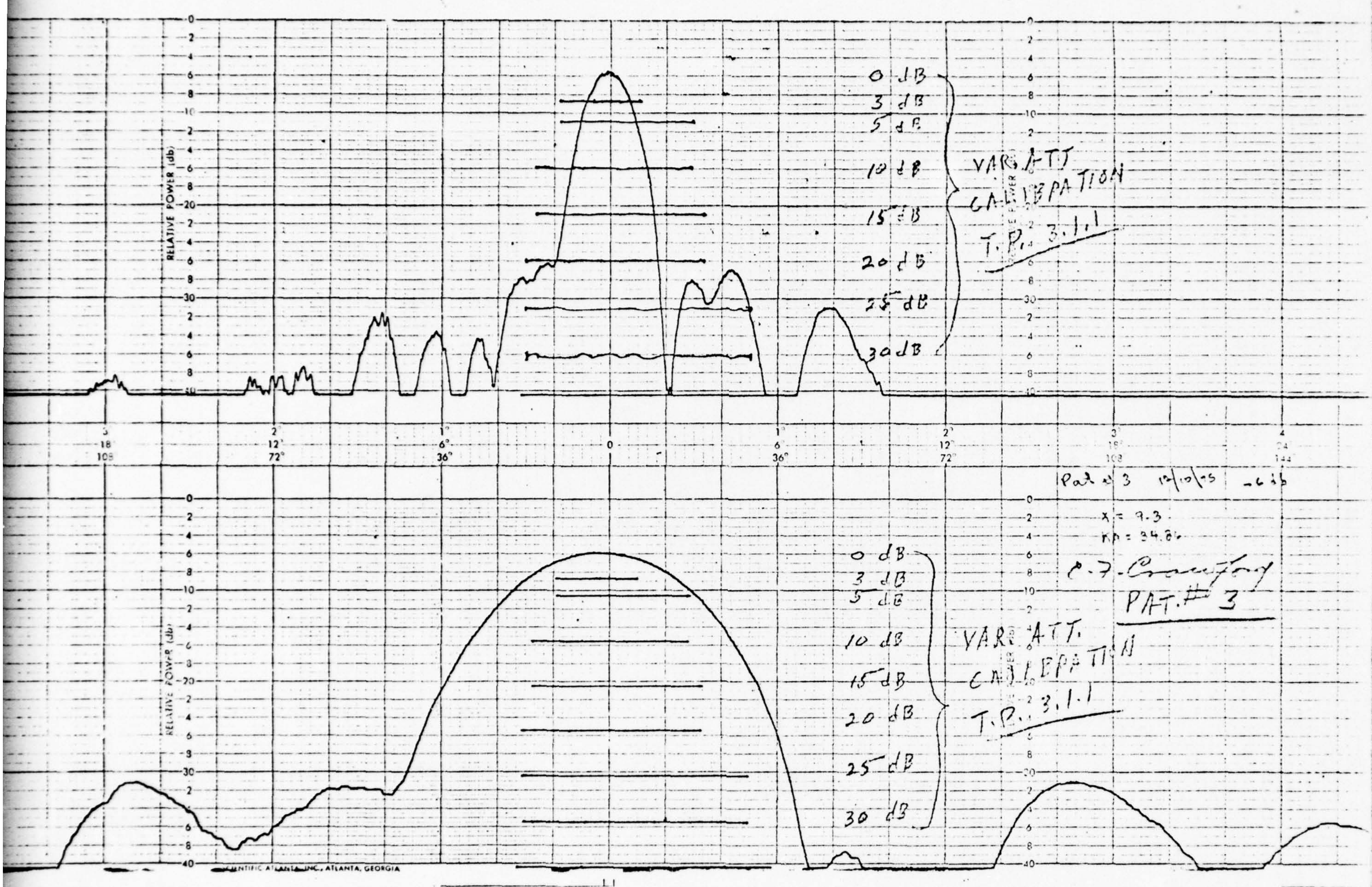
0 dB
3 dB
5 dB
10 dB
15 dB
20 dB
25 dB
30 dB
VAR. ATT.
CALIBRATION
T.P. 3.1.1
RELATIVE POWER (db)
Pat # 3 12/10/75 -6 db
x = 9.3
RP = 34.86
PAT. # 3
SCIENTIFIC ATLANTA INC., ATLANTA, GEORGIA
L1

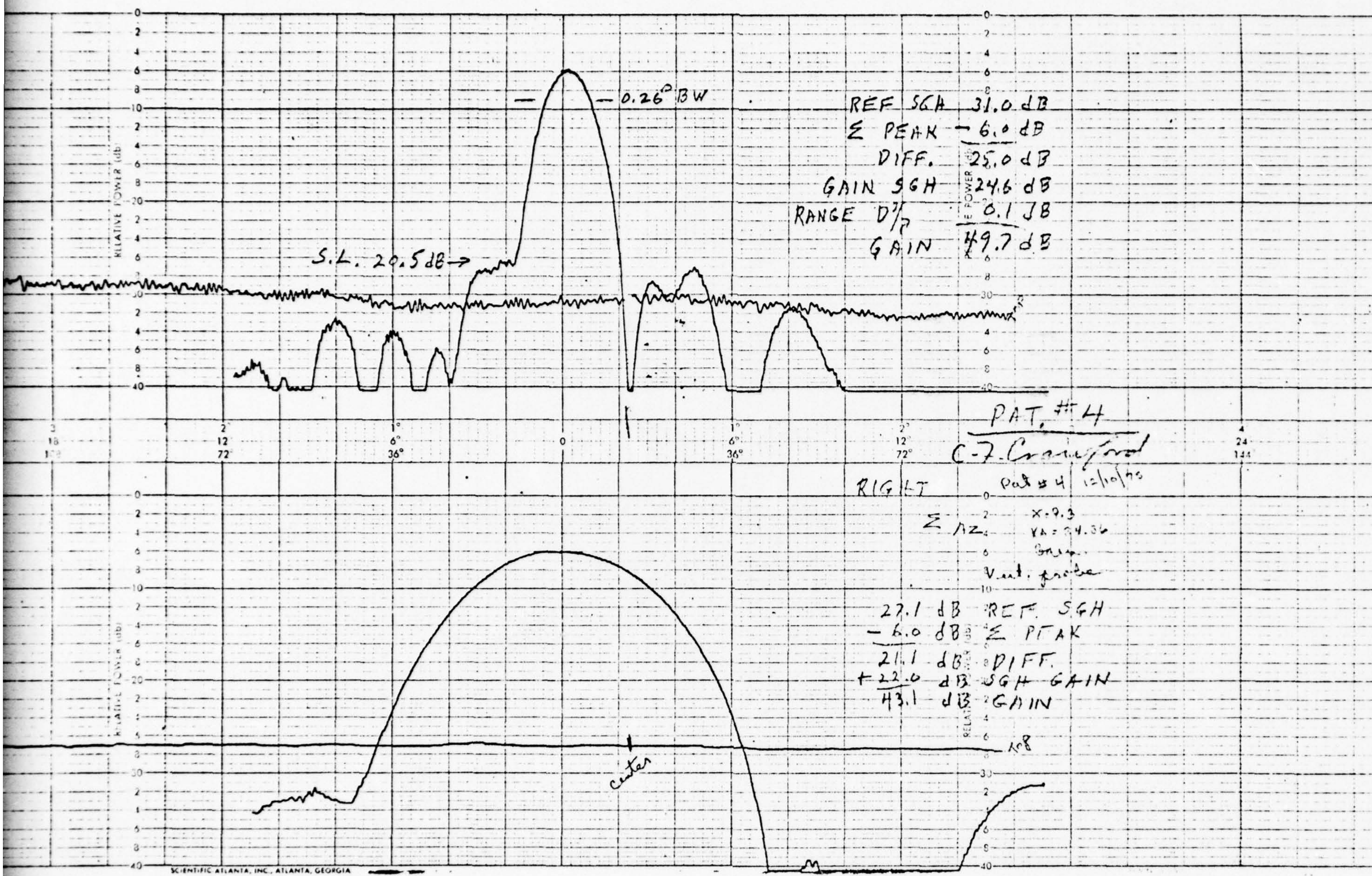

0.26° BW
S.L. 20.5 dB
REF SGH 31.0 dB
Σ PEAK − 6.0 dB
DIFF. 25.0 dB
GAIN SGH 24.6 dB
RANGE D/P 0.1 dB
GAIN 49.7 dB
PAT. #4
C-7 Crawford
RIGHT
Σ AZ.
Pat #4 12/10/75
27.1 dB REF. SGH
− 6.0 dB Σ PEAK
21.1 dB DIFF.
+ 22.0 dB SGH GAIN
43.1 dB GAIN
center
RELATIVE POWER (db)
SCIENTIFIC ATLANTA, INC., ATLANTA, GEORGIA

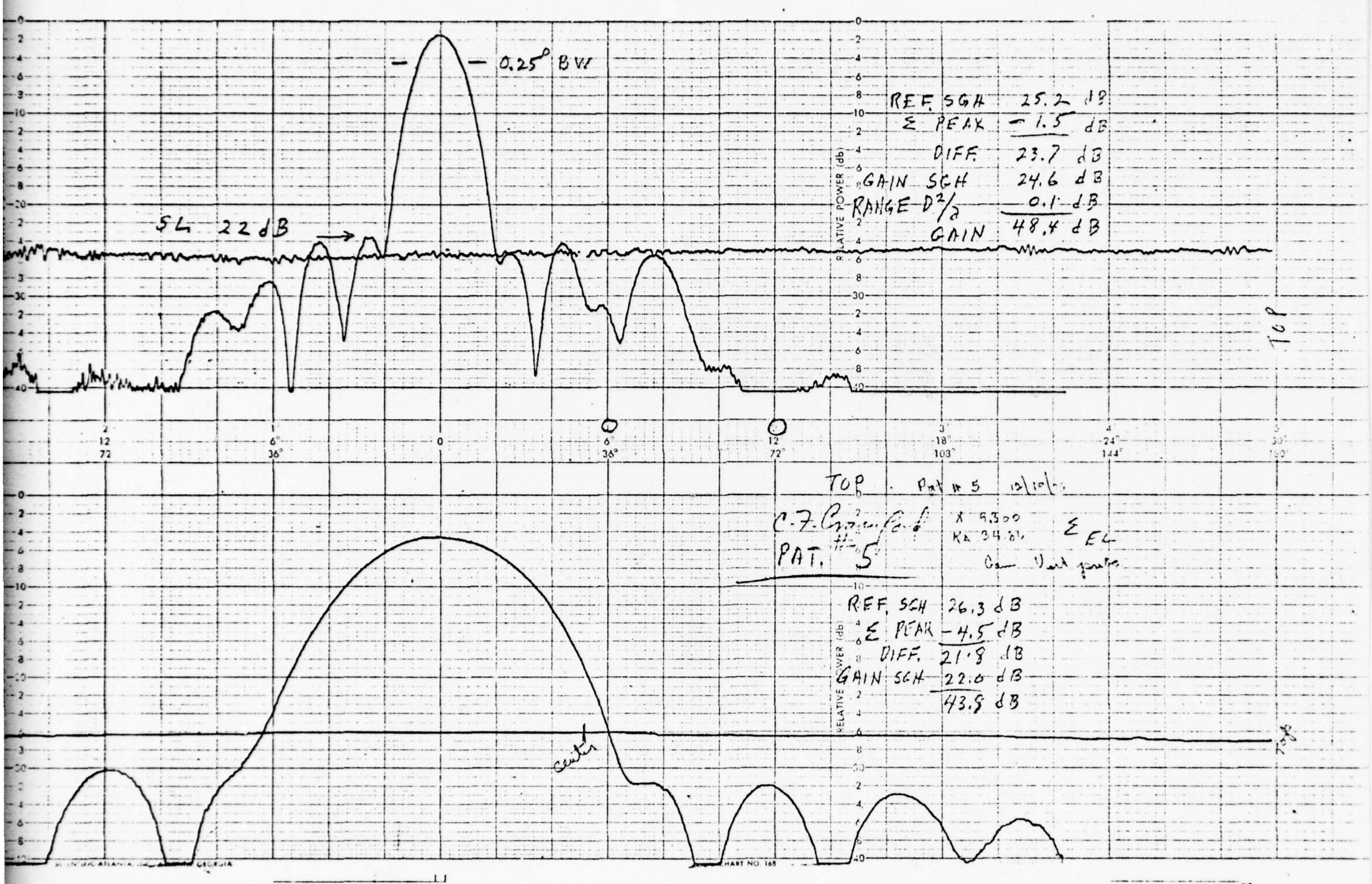

0.25° BW
SL 22 dB
REF. SGH 25.2 dB
Σ PEAK -1.5 dB
DIFF. 23.7 dB
GAIN SGH 24.6 dB
RANGE D²/2 0.1 dB
GAIN 48.4 dB
RELATIVE POWER (db)
TOP
TOP Pat # 5
PAT. # 5
Σ EL
REF. SGH 26.3 dB
Σ PEAK -4.5 dB
DIFF. 21.8 dB
GAIN SGH 22.0 dB
43.8 dB
center
CHART NO. 168

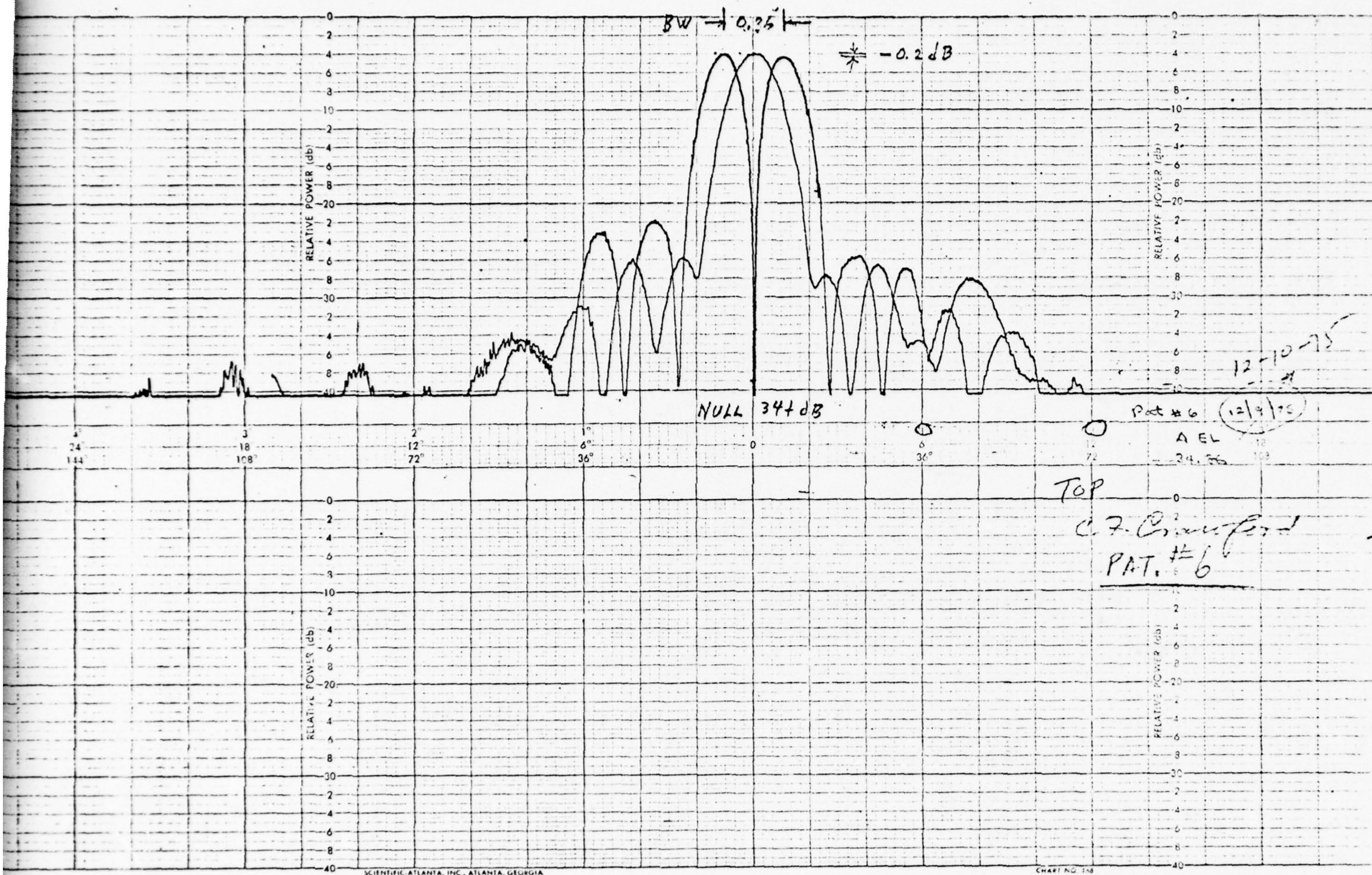
BW 0.25°
-0.2 dB
NULL 34+dB
RELATIVE POWER (db)
Pat #6 12/9/75
Δ EL
34.36
12-10-75
TOP
C. F. Crawford
PAT. #6
SCIENTIFIC-ATLANTA, INC., ATLANTA, GEORGIA

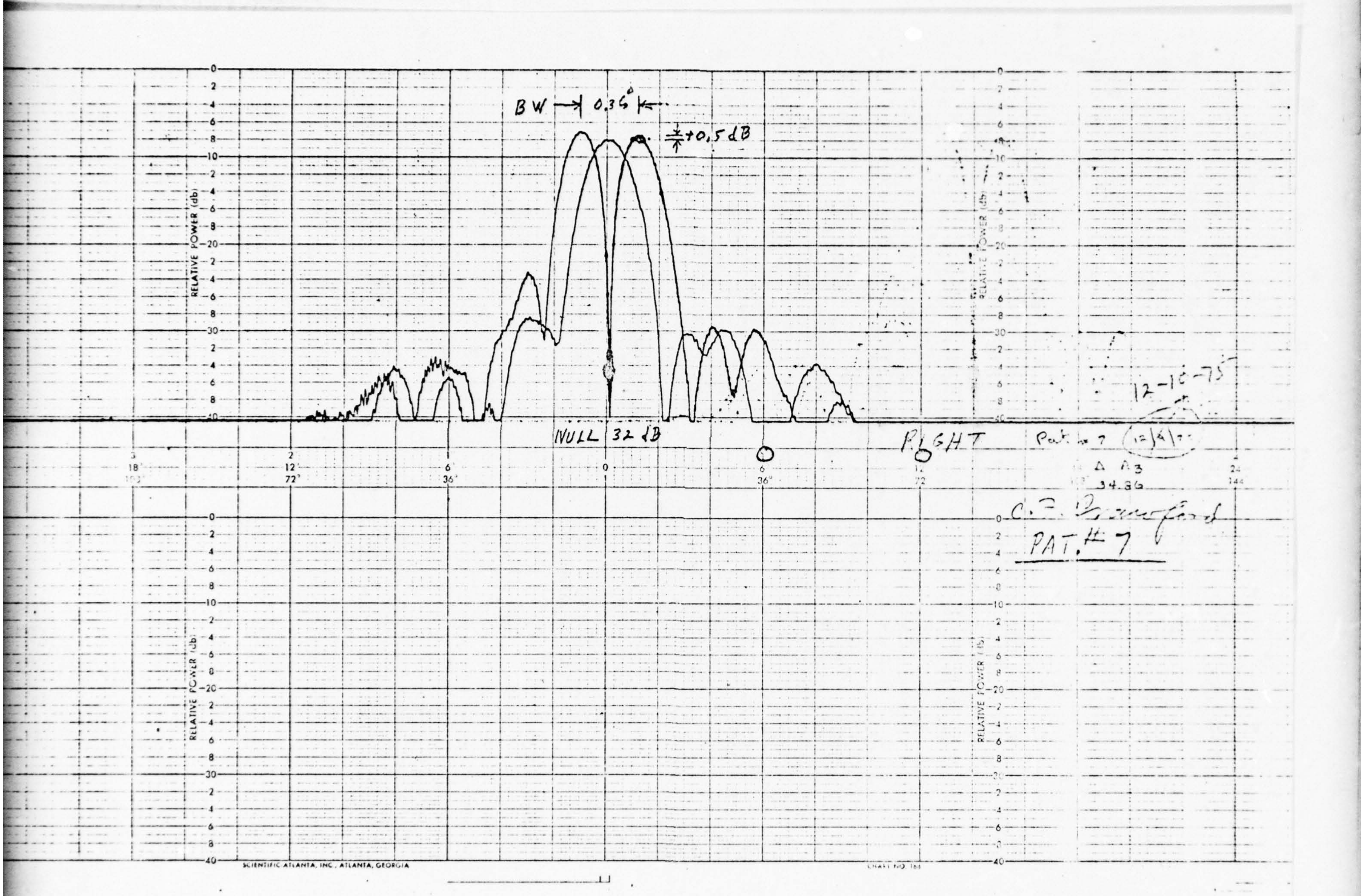
BW → 0.36° ←
+0.5 dB
NULL 32 dB
RIGHT
12-18-75
Pat. 7
Δ A3
34.36
C. F. Crawford
PAT. # 7
RELATIVE POWER (db)
SCIENTIFIC ATLANTA, INC., ATLANTA, GEORGIA

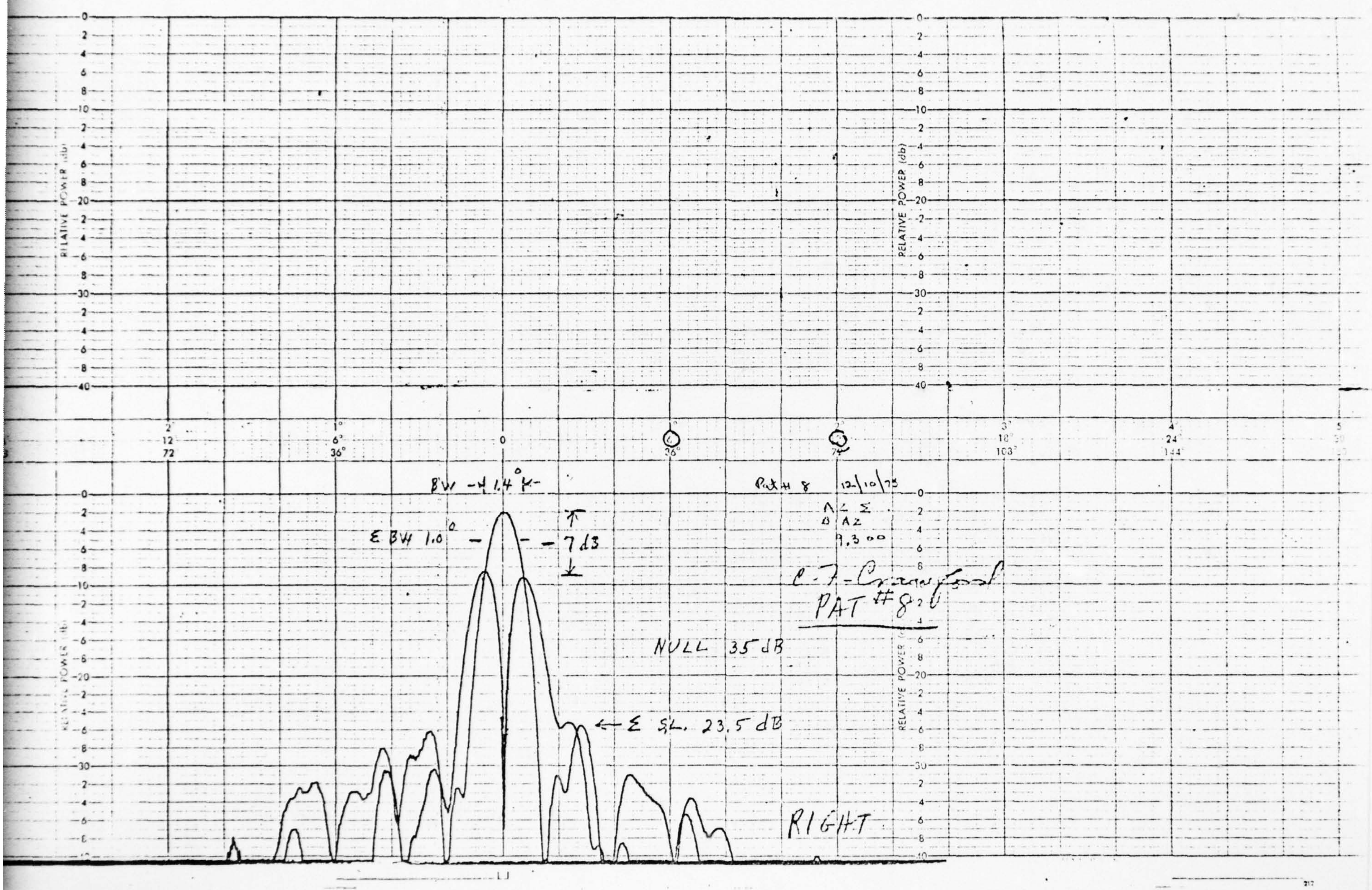

RELATIVE POWER (db)
BW ~1.4°
Σ BW 1.0°
7 dB
Path 8 12/10/73
Δ ⊥ Σ
Δ AZ
9,300
NULL 35 dB
← Σ SL. 23.5 dB
RIGHT
PAT #8

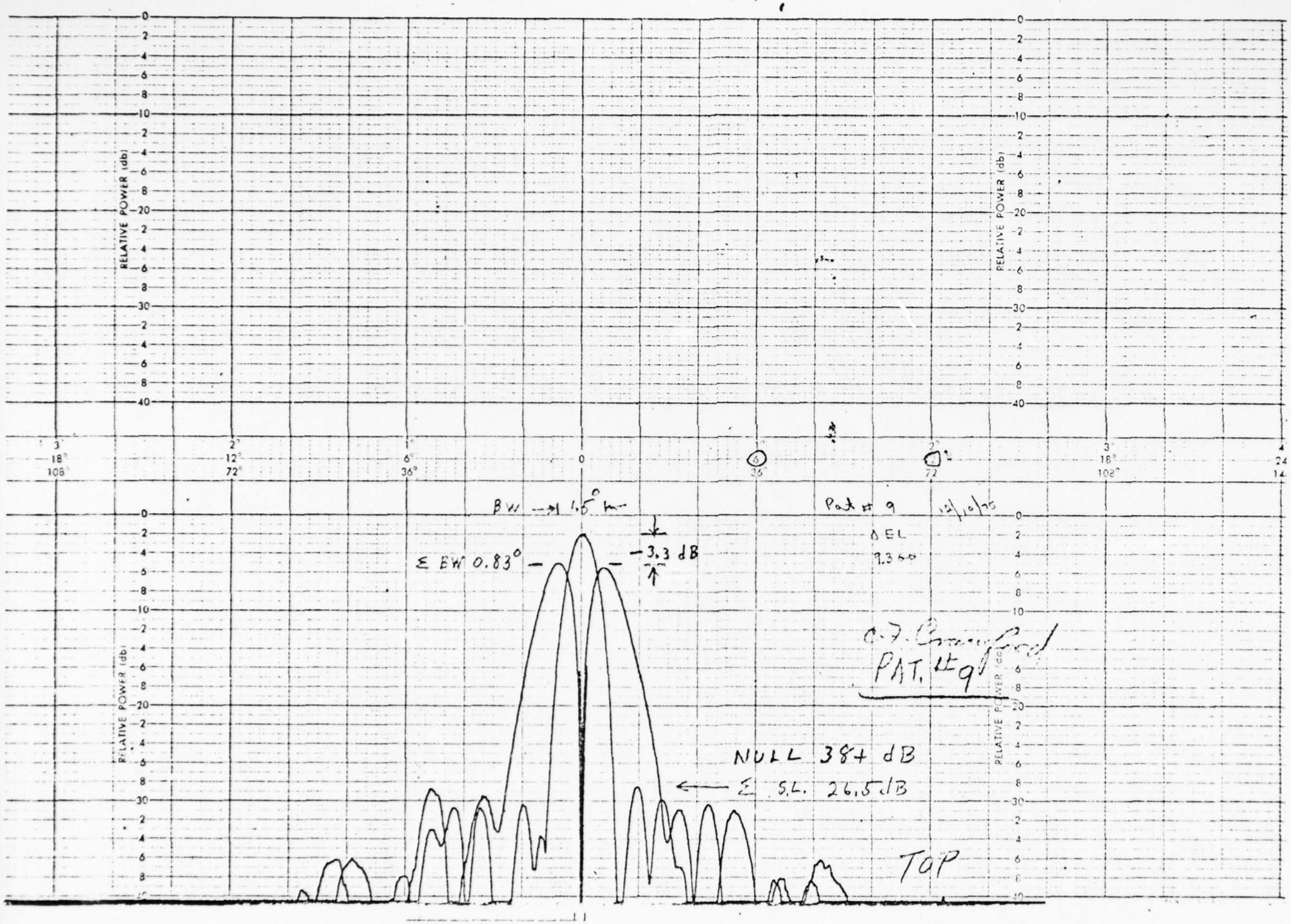

RELATIVE POWER (db)
0
10
20
30
40
BW 1.5°
Σ BW 0.83°
3.3 dB
Pat # 9
12/10/75
Δ EL
9.36
C.J. Crawford
PAT. #9
NULL 38+ dB
Σ S.L. 26.5 dB
TOP

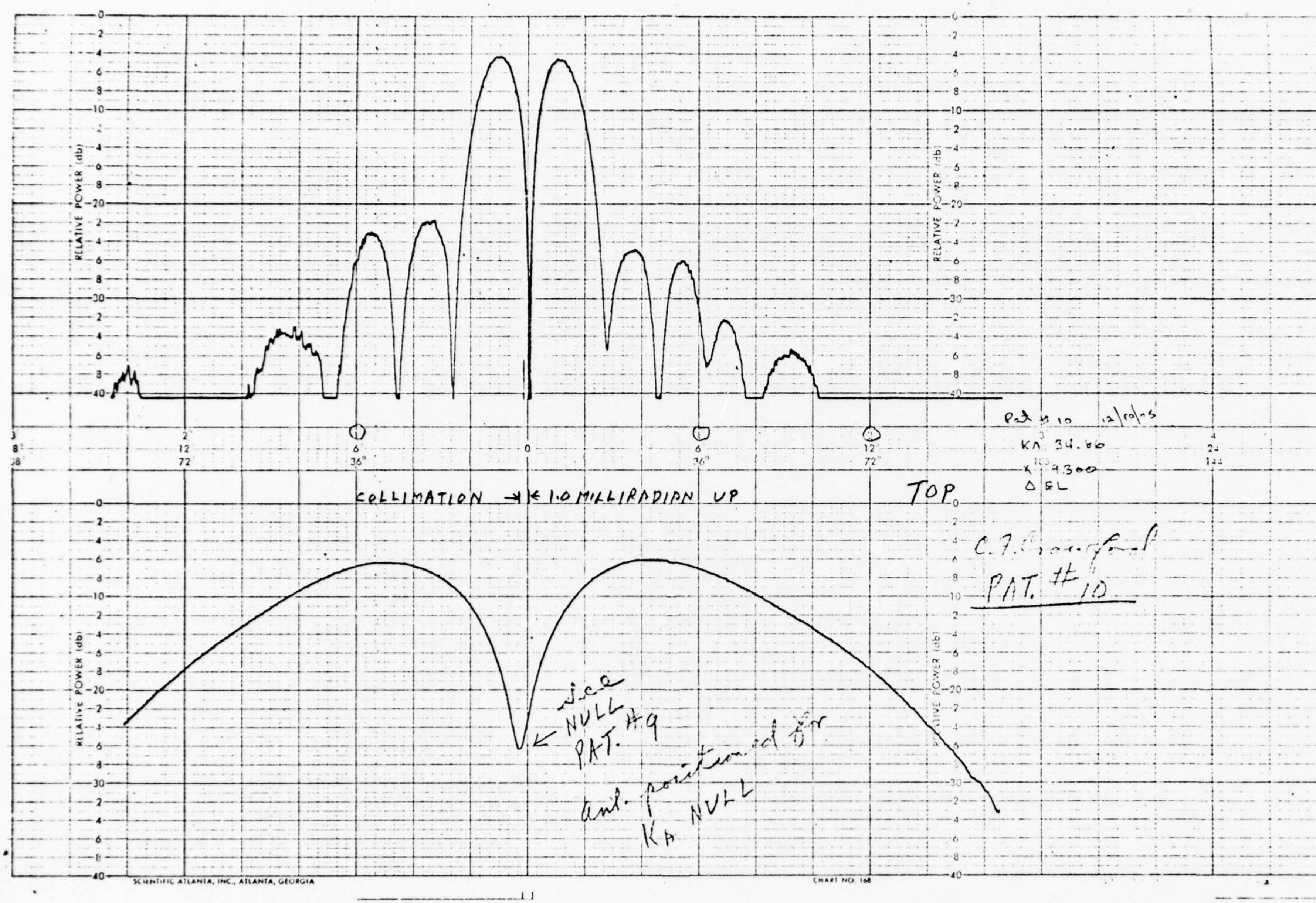
RELATIVE POWER (db)
COLLIMATION →|← 1.0 MILLIRADIAN UP
TOP
Pat # 10 12/10/75
KA 34.86
X 9.300
Δ EL
PAT. # 10
see NULL PAT. #9
Ant. positioned for KA NULL
SCIENTIFIC ATLANTA, INC., ATLANTA, GEORGIA
CHART NO. 168

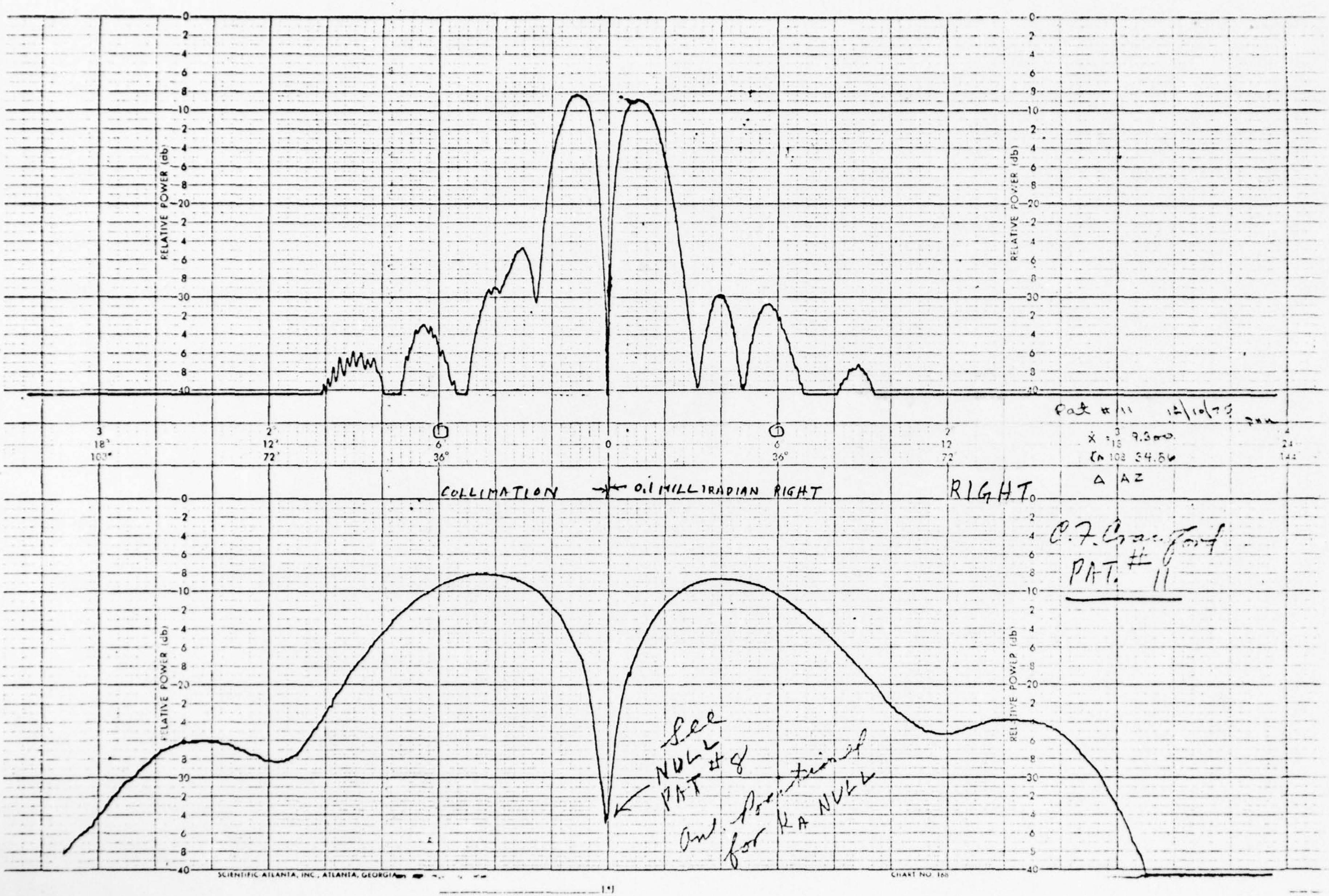
RELATIVE POWER (db)
COLLIMATION → 0.1 MILLIRADIAN RIGHT
RIGHT
Pat # 11 12/10/73
Δ AZ
C.F. Crawford
PAT. # 11
See NULL PAT # 8
Ant. Positioned for KA NULL
SCIENTIFIC ATLANTA, INC., ATLANTA, GEORGIA
CHART NO. 166

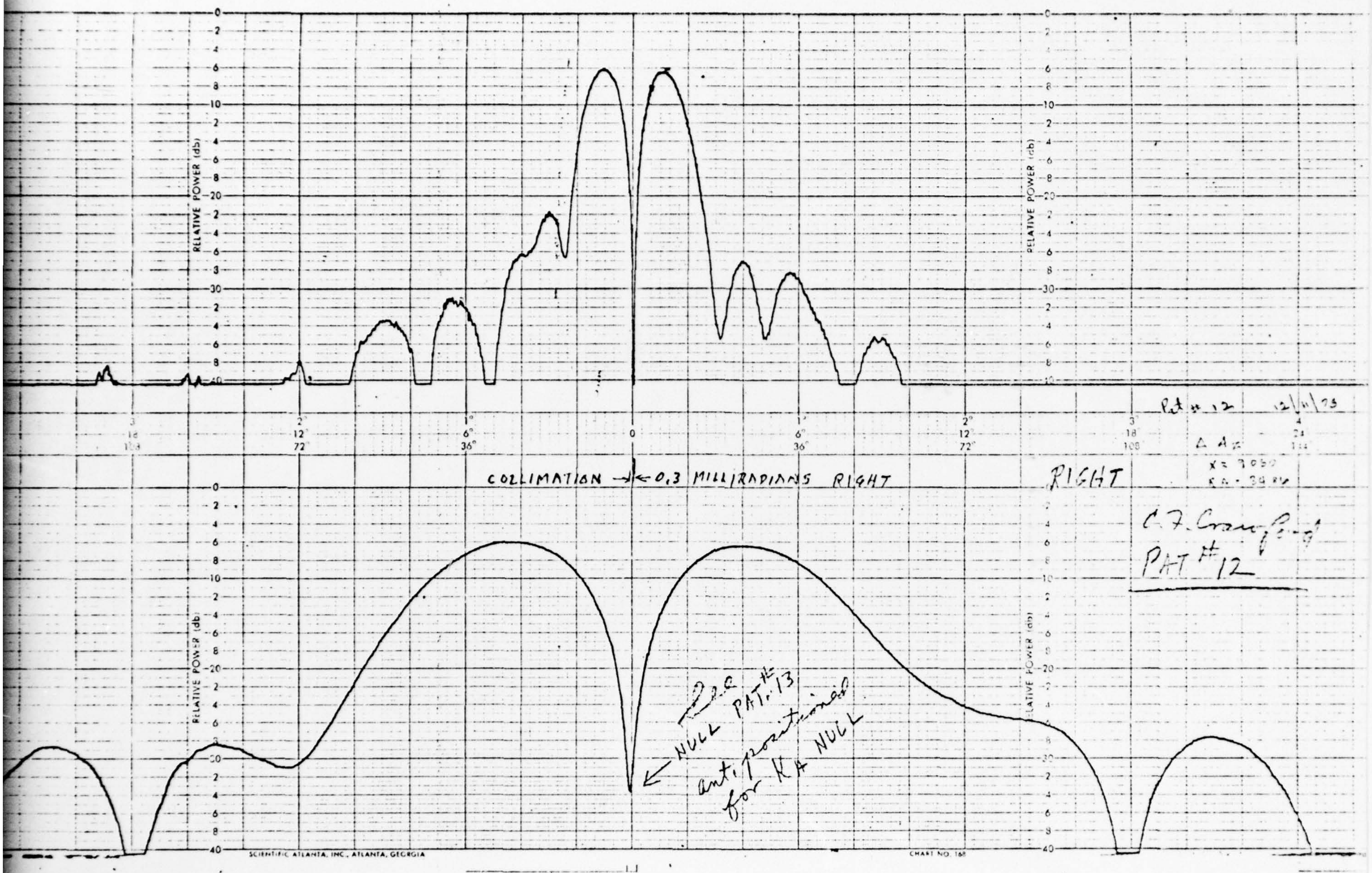
RELATIVE POWER (db)
COLLIMATION → ← 0.3 MILLIRADIANS RIGHT
RIGHT
Pat # 12 12/11/73
PAT # 12
NULL PAT. 13
anti positioned for KA NULL
SCIENTIFIC ATLANTA, INC., ATLANTA, GEORGIA
CHART NO. 168

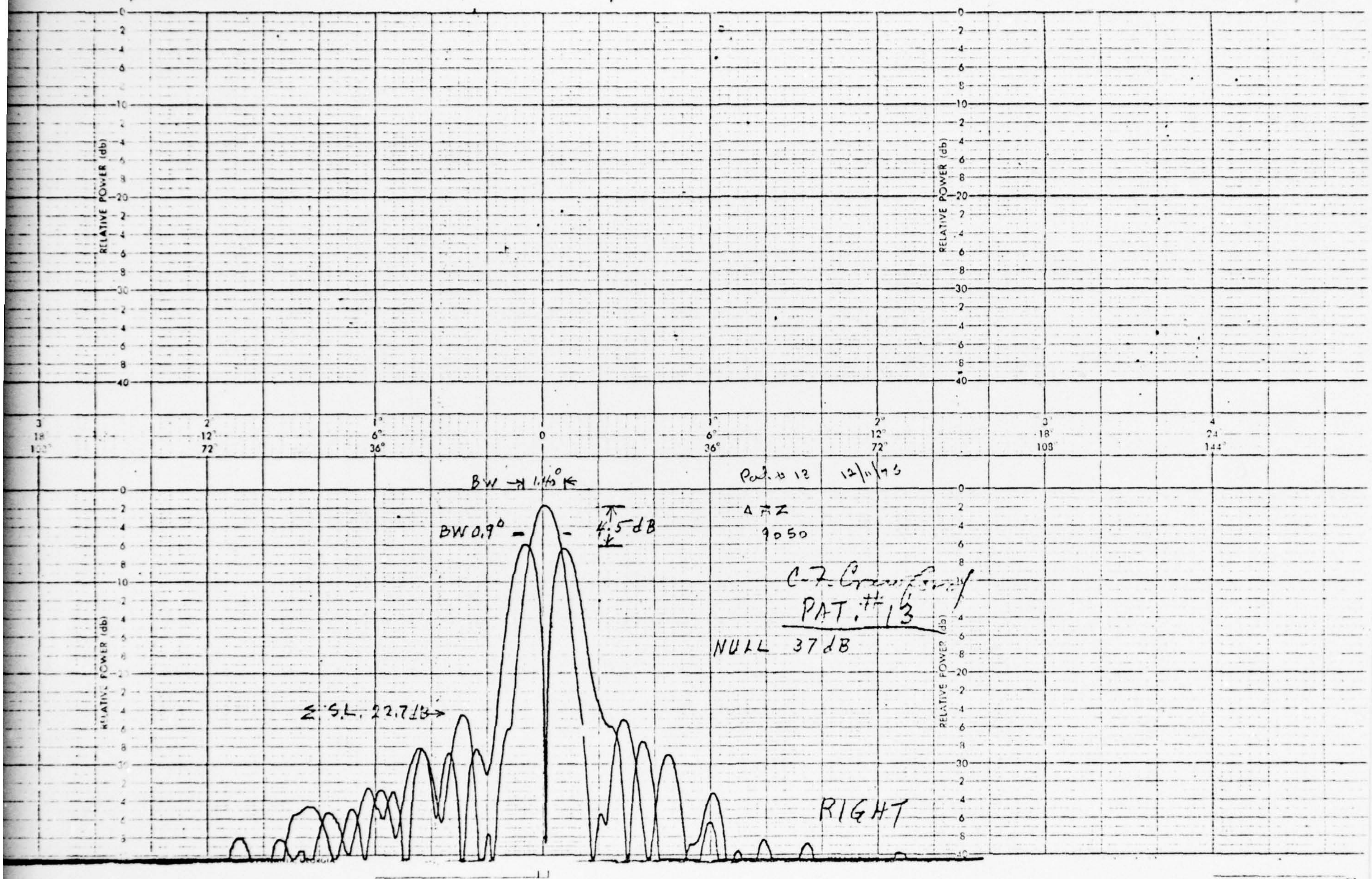

BW → 1.40° ←
BW 0.9°
4.5 dB
Pat. # 12 12/11/73
AZ
9050
C. F. Crawford
PAT. # 13
NULL 37 dB
Σ S.L. 22.7 dB →
RIGHT
RELATIVE POWER (db)

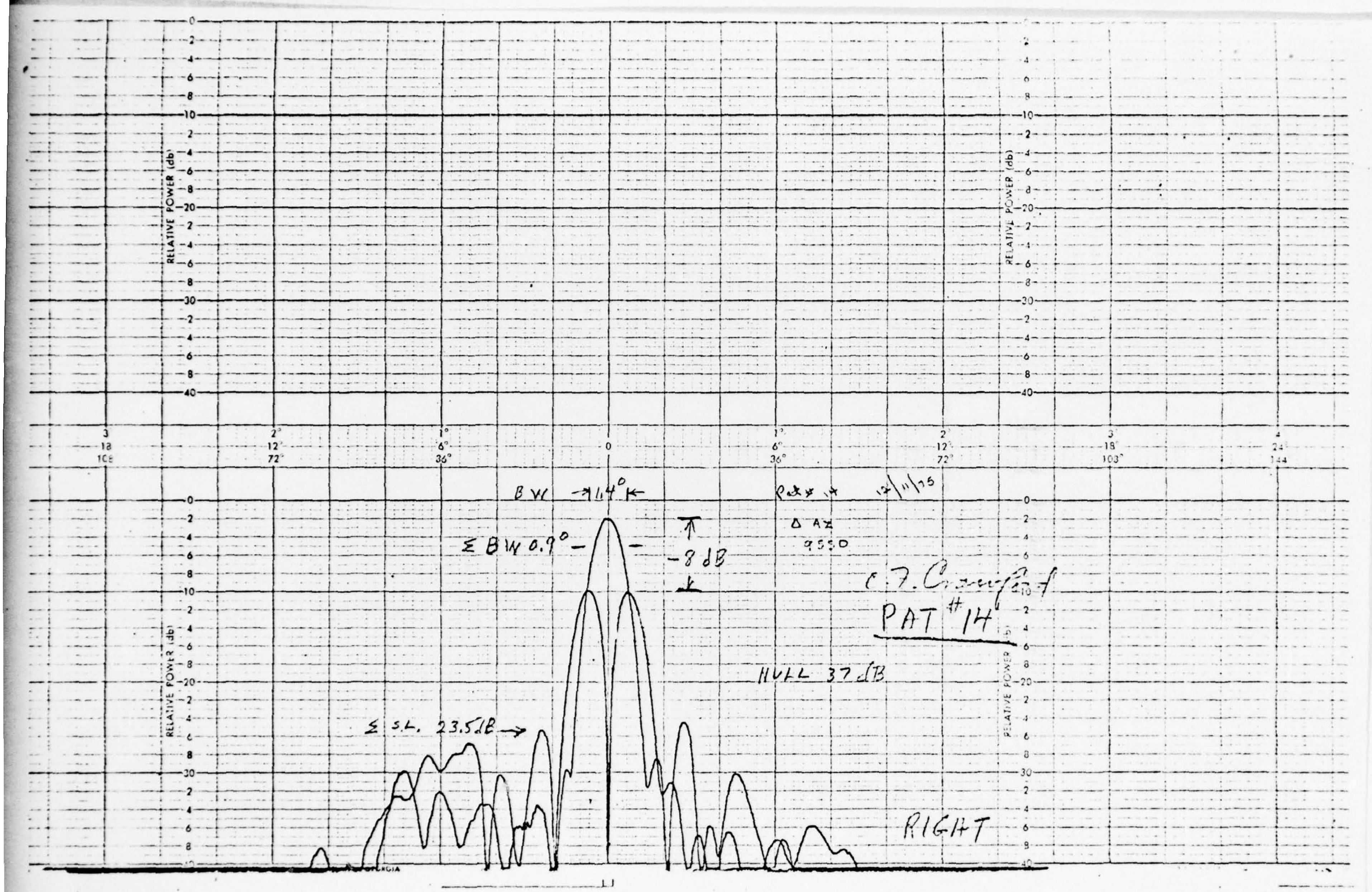

BW →1.4° ←
Pat # 14 12/11/75
Σ BW 0.9°
-8 dB
Δ AZ
95.50
C. T. Crawford
PAT # 14
NULL 37 dB
Σ S.L. 23.5 dB →
RIGHT
RELATIVE POWER (db)

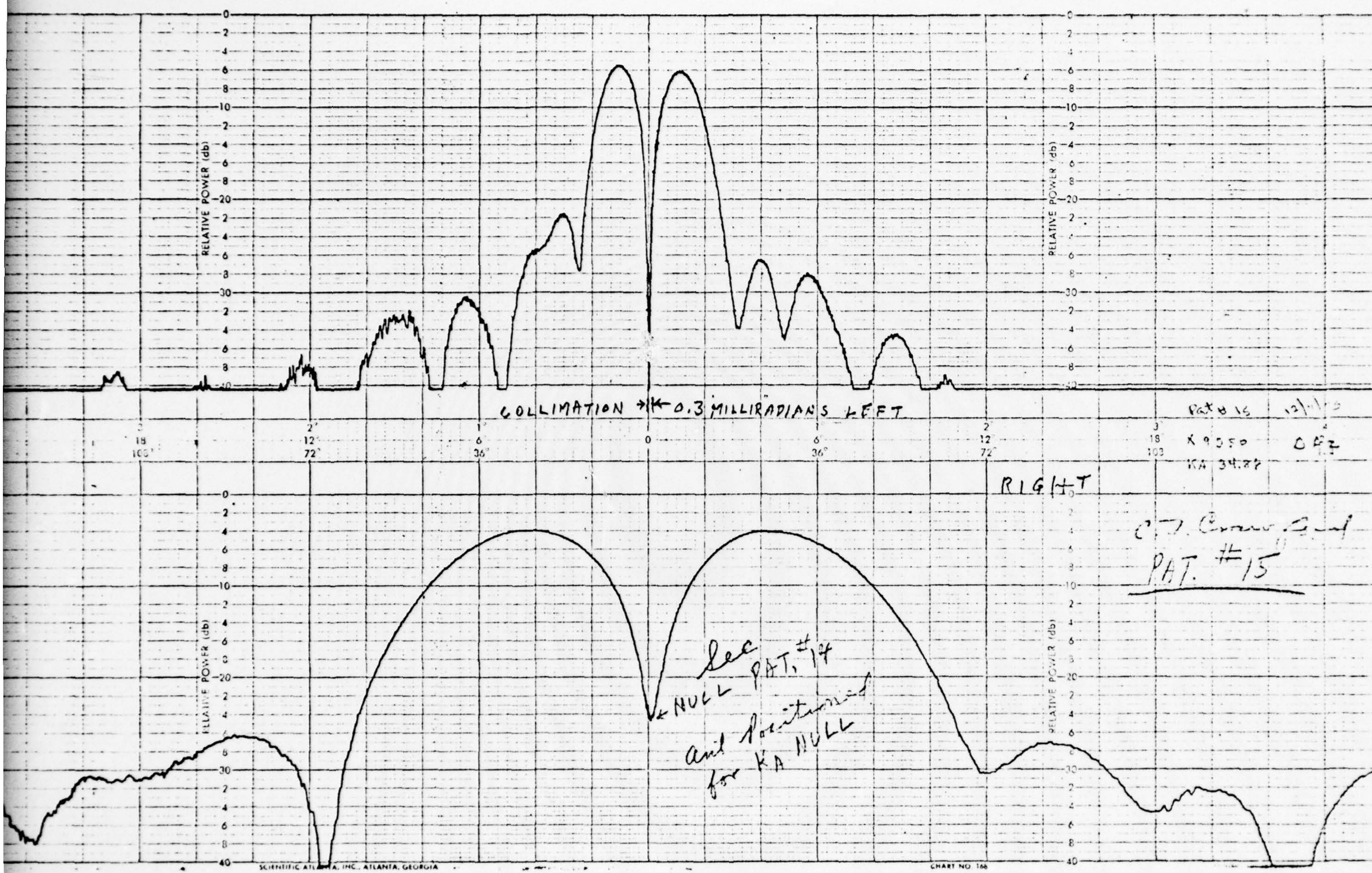
RELATIVE POWER (db)
COLLIMATION → ← 0.3 MILLIRADIANS LEFT
RIGHT
Pat # 15
K 9350
KA 34.87
C.J. Crawford
PAT. #15
See PAT. #14
← NULL
and Positioned for KA NULL
SCIENTIFIC ATLANTA, INC., ATLANTA, GEORGIA
CHART NO 166

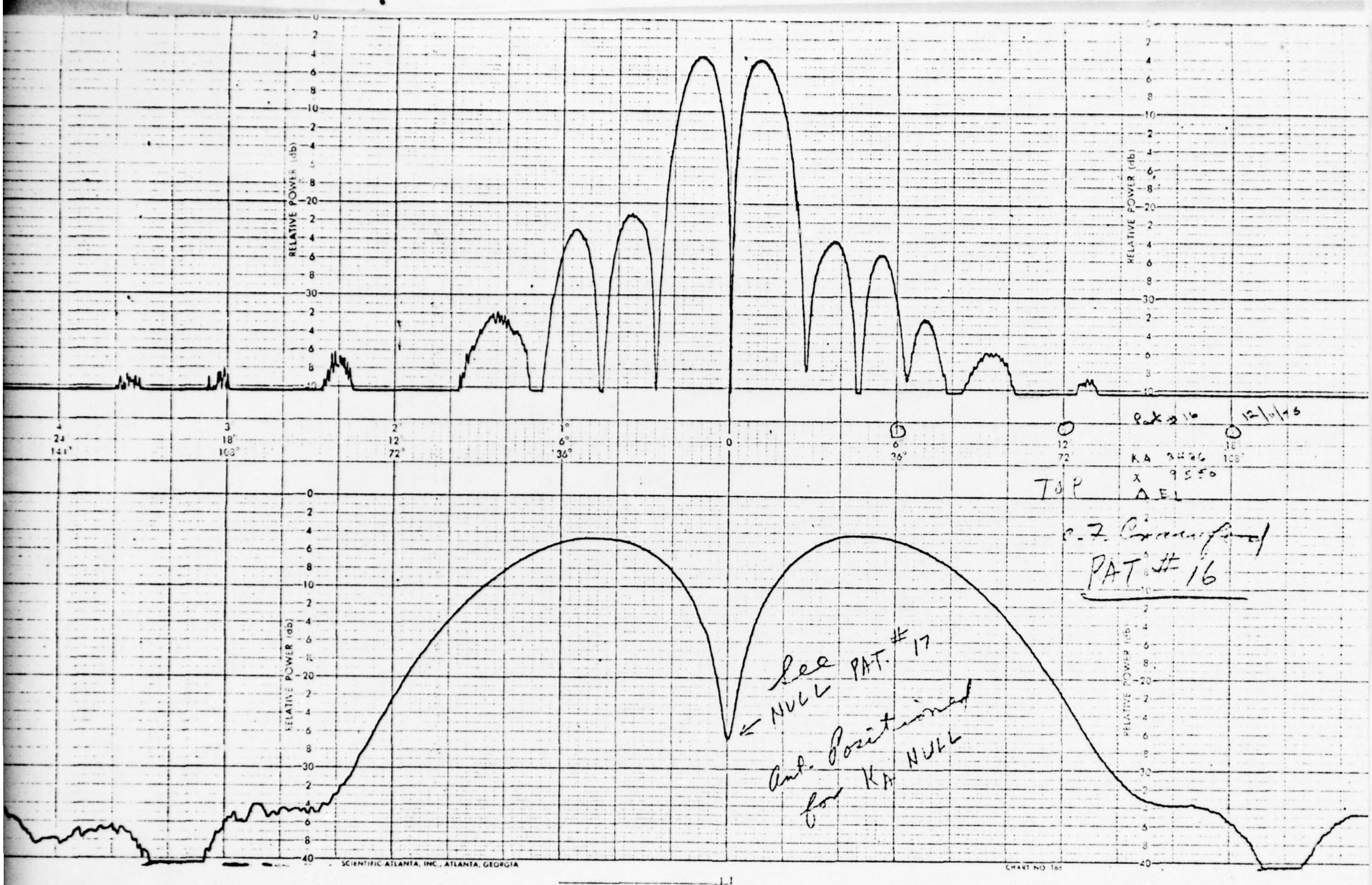
RELATIVE POWER (db)
Pat # 16
12/1/75
KA 3436
X 9550
Δ EL
TOP
PAT # 16
See PAT # 17
← NULL
Ant. Positioned for KA NULL
SCIENTIFIC ATLANTA, INC., ATLANTA, GEORGIA

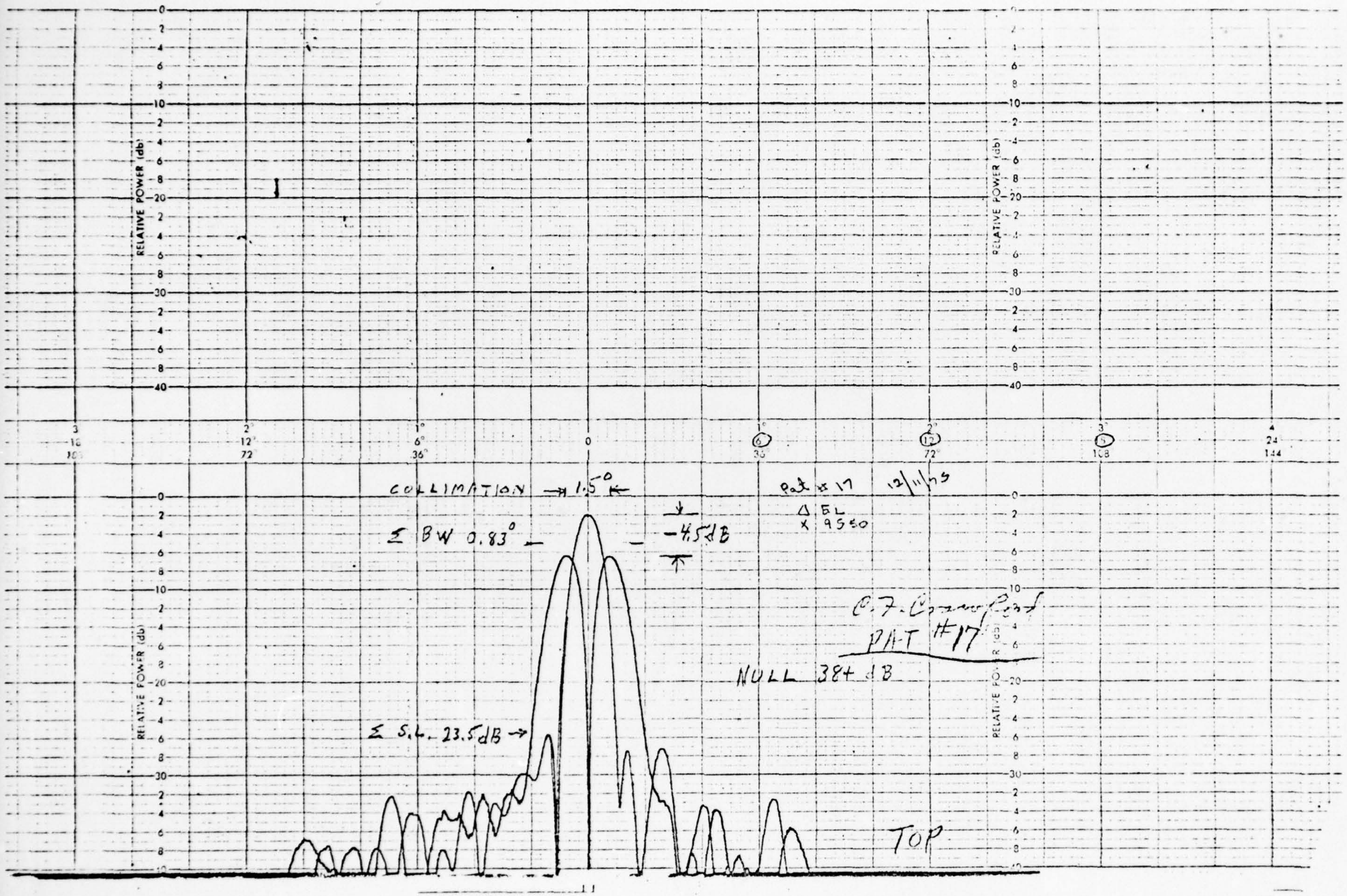
RELATIVE POWER (db)
COLLIMATION → 1.5° ←
Σ BW 0.83°
-4.5 dB
Pat # 17 12/11/75
Δ EL
X 9550
C.F. Crawford
PAT #17
NULL 38+ dB
Σ S.L. 23.5 dB →
TOP

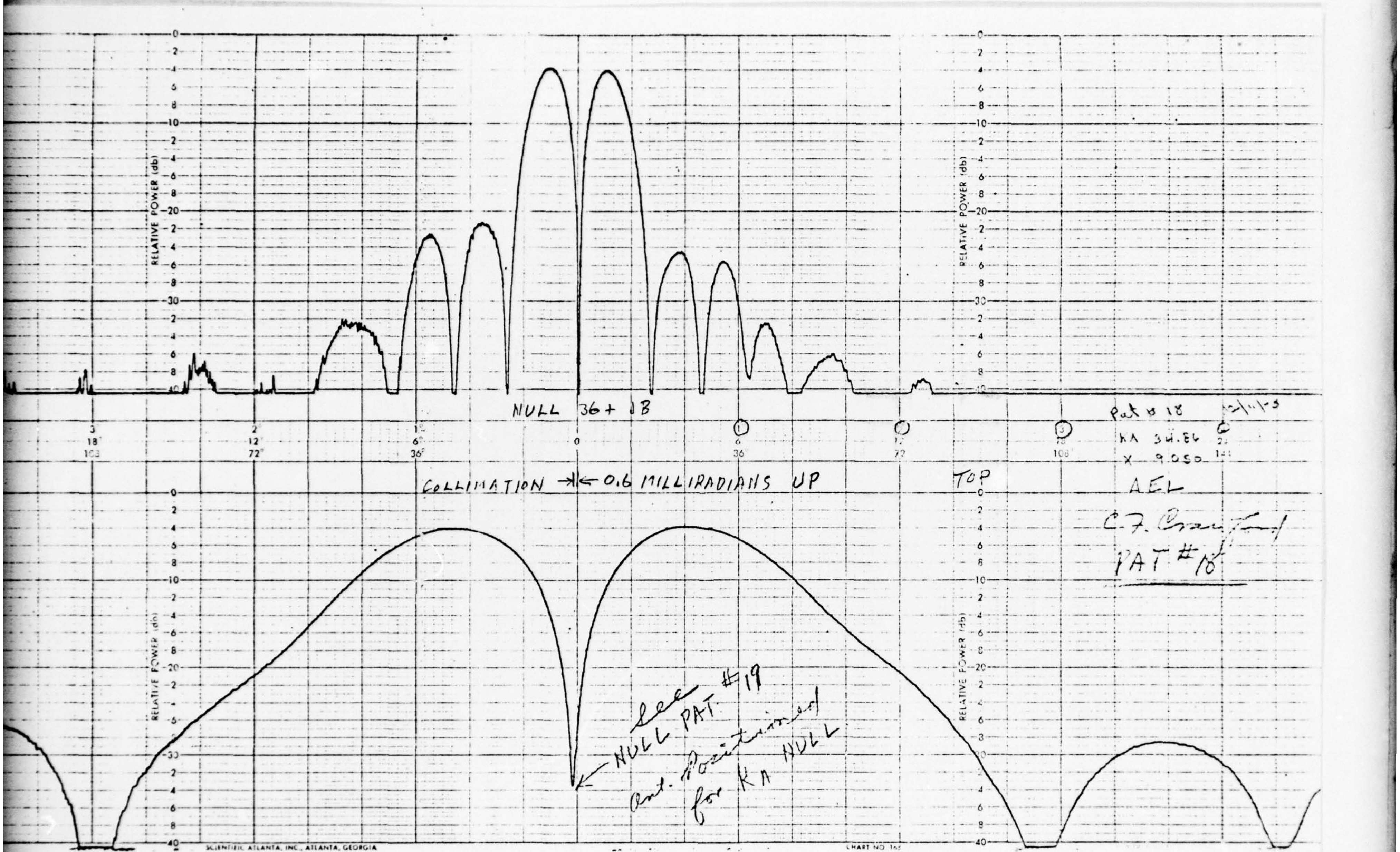

RELATIVE POWER (db)
NULL 36+ dB
Pat # 18
KA 34.86
X 9.050
COLLIMATION →|← 0.6 MILLIRADIANS UP
TOP
AEL
C.F. Crawford
PAT # 18
See NULL PAT #19
Ant. Positioned for KA NULL
SCIENTIFIC ATLANTA, INC., ATLANTA, GEORGIA
CHART NO. 165

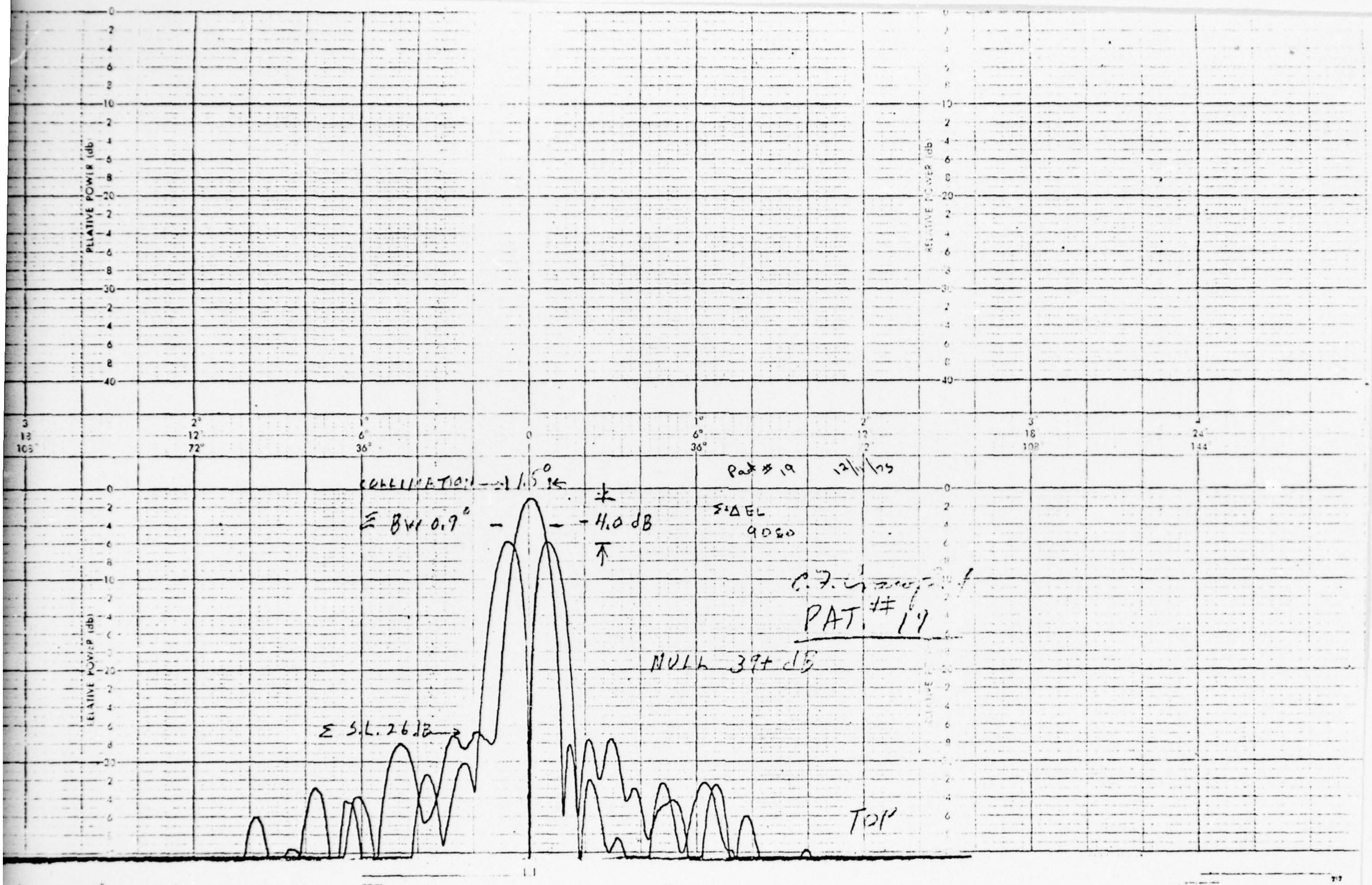
RELATIVE POWER (db)
Pat # 19 12/1/75
COLLIMATION ~1.5°
Σ BW 0.9°
4.0 dB
ΣΔ EL
9080
PAT # 19
NULL 39+ dB
Σ S.L. 26 dB
TOP

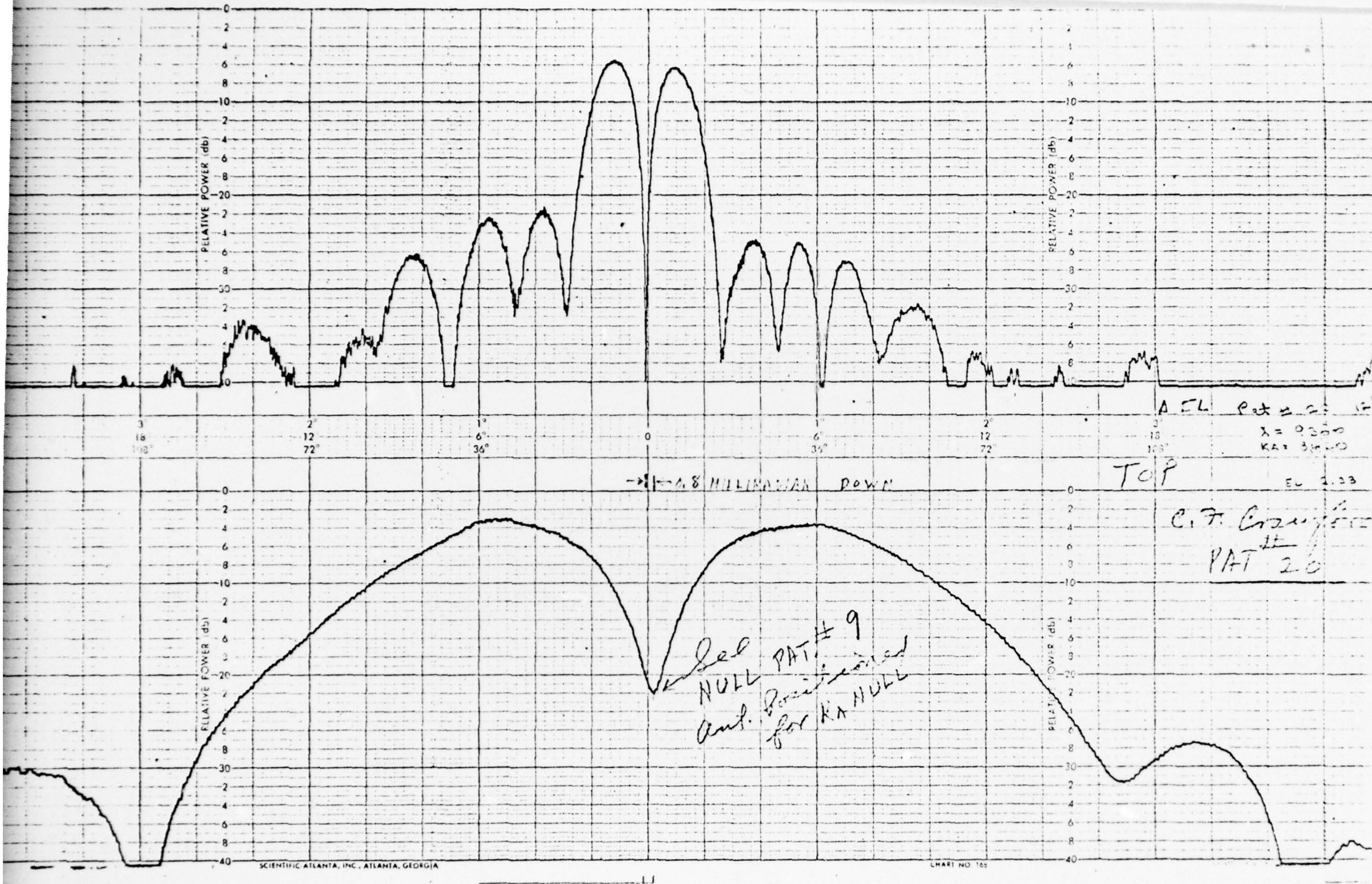

RELATIVE POWER (db)
TOP
C. F. Crawford
PAT # 26
See NULL PAT # 9
SCIENTIFIC ATLANTA, INC., ATLANTA, GEORGIA

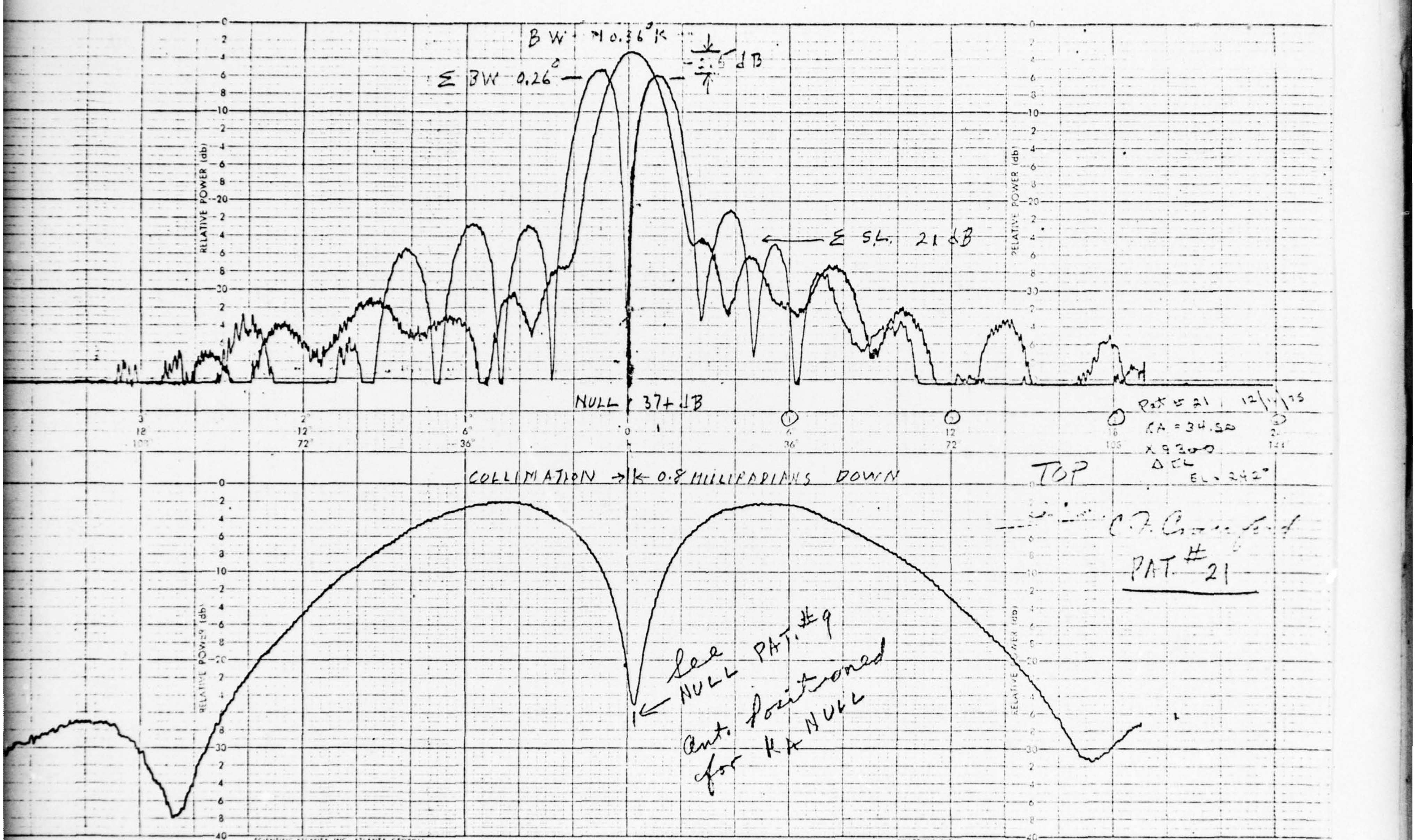
BW 0.36°
Σ BW 0.26°
dB
Σ SL. 21 dB
NULL 37+ dB
Pat # 21
COLLIMATION → ← 0.8 MILLIRADIANS DOWN
TOP
PAT # 21
See NULL PAT. #9
Ant. Positioned for RA NULL
RELATIVE POWER (db)
SCIENTIFIC ATLANTA, INC., ATLANTA, GEORGIA
CHART NO. 168

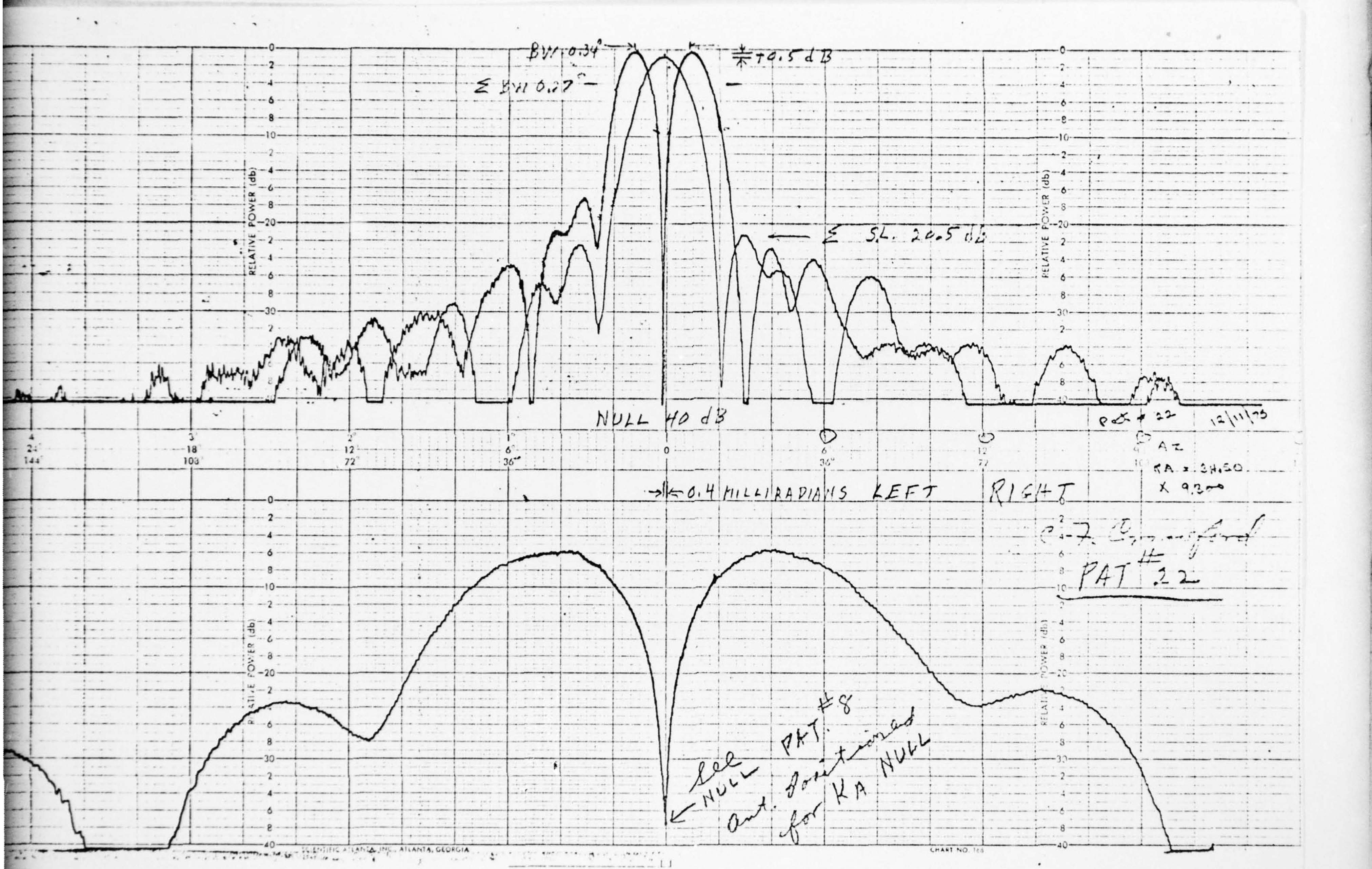

BW 0.34°
Σ BW 0.27°
∓ 40.5 dB
Σ SL. 20.5 dB
NULL 40 dB
RELATIVE POWER (db)
0.4 MILLIRADIANS LEFT RIGHT
PAT # 22
12/11/73
AZ
KA = 34.50
X 9.3
PAT # 22
See NULL PAT. # 8
Ant. positioned for KA NULL
SCIENTIFIC ATLANTA, INC. ATLANTA, GEORGIA
CHART NO. 166

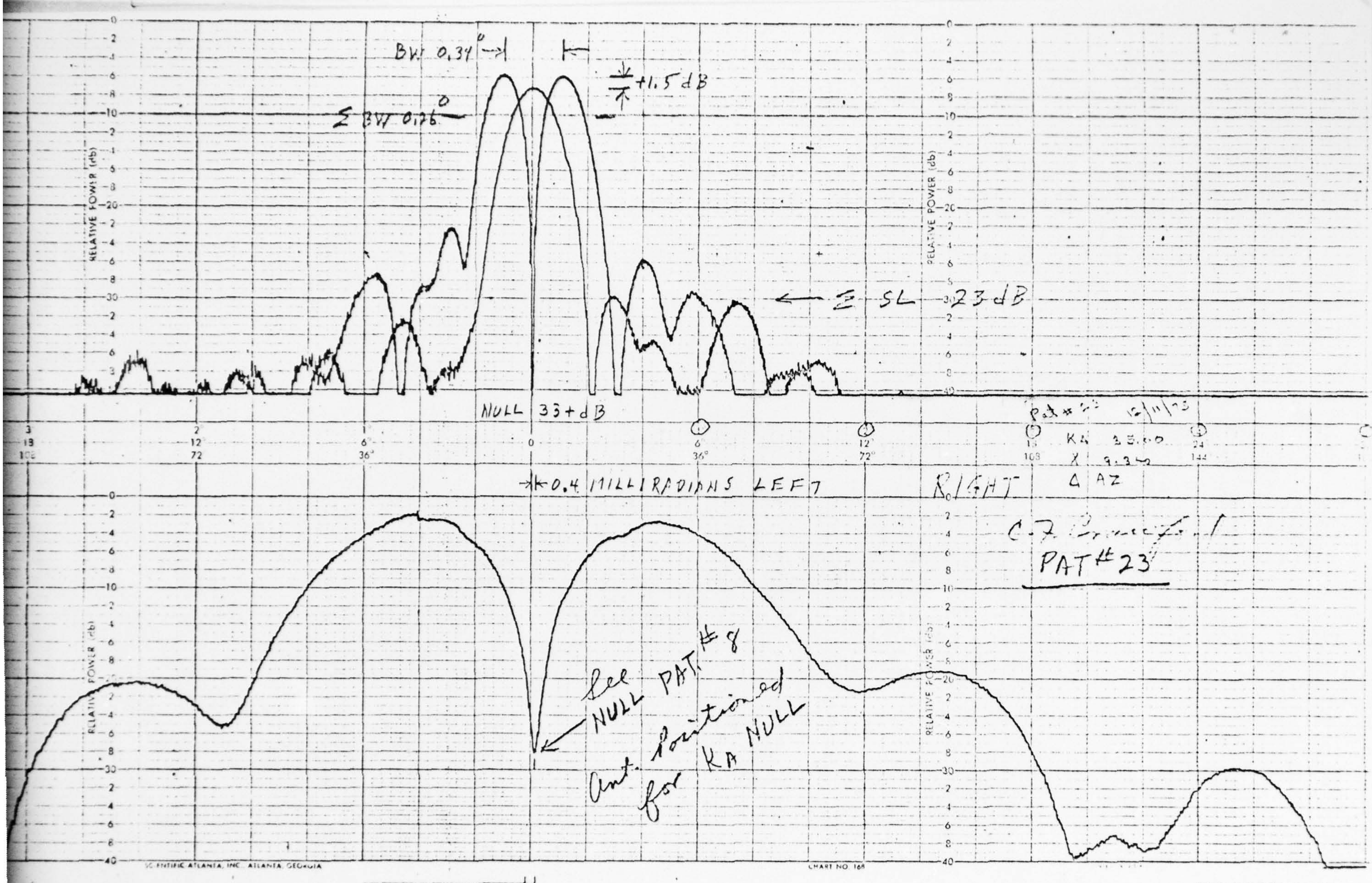

BW 0.34°
Σ BW 0.26°
+1.5 dB
Σ SL 23 dB
NULL 33+ dB
0.4 MILLIRADIANS LEFT
RIGHT
KA
Δ AZ
PAT # 23
See NULL PAT # 8
Ant. Positioned for KA NULL
RELATIVE POWER (db)
SCIENTIFIC ATLANTA, INC. ATLANTA, GEORGIA
CHART NO. 168

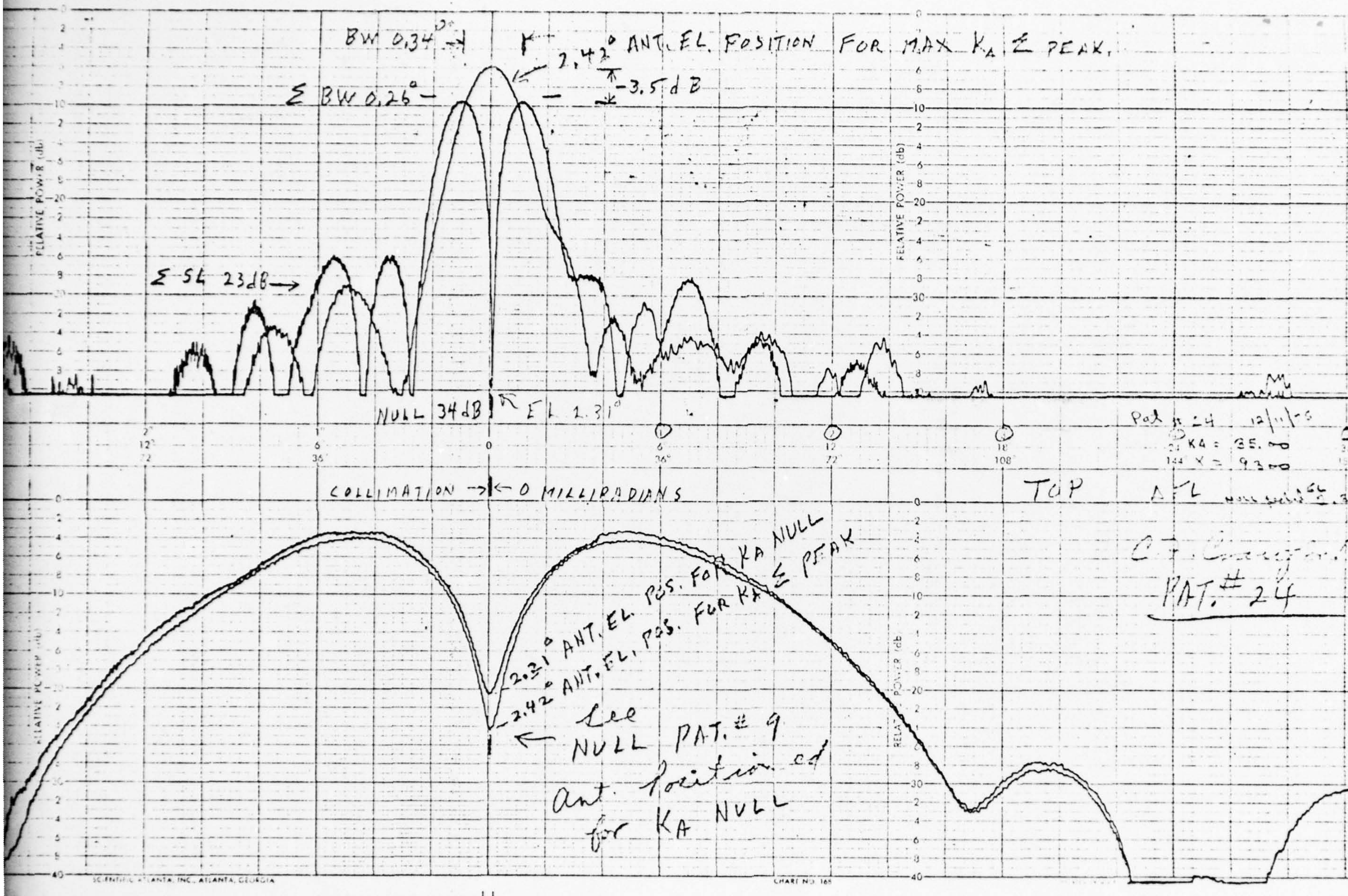
BW 0.34°
2.42° ANT. EL. POSITION FOR MAX K_A Σ PEAK.
Σ BW 0.26°
-3.5 dB
Σ SL 23dB
NULL 34dB
EL 1.31°
COLLIMATION → ← 0 MILLIRADIANS
TOP
Pat # 24
KA = 35.
X = 9.3
2.31° ANT. EL. POS. FOR KA NULL
2.42° ANT. EL. POS. FOR KA Σ PEAK
See NULL PAT. # 9
Ant. position ed for KA NULL
PAT. # 24
RELATIVE POWER (db)
SCIENTIFIC ATLANTA, INC., ATLANTA, GEORGIA
CHART NO. 165

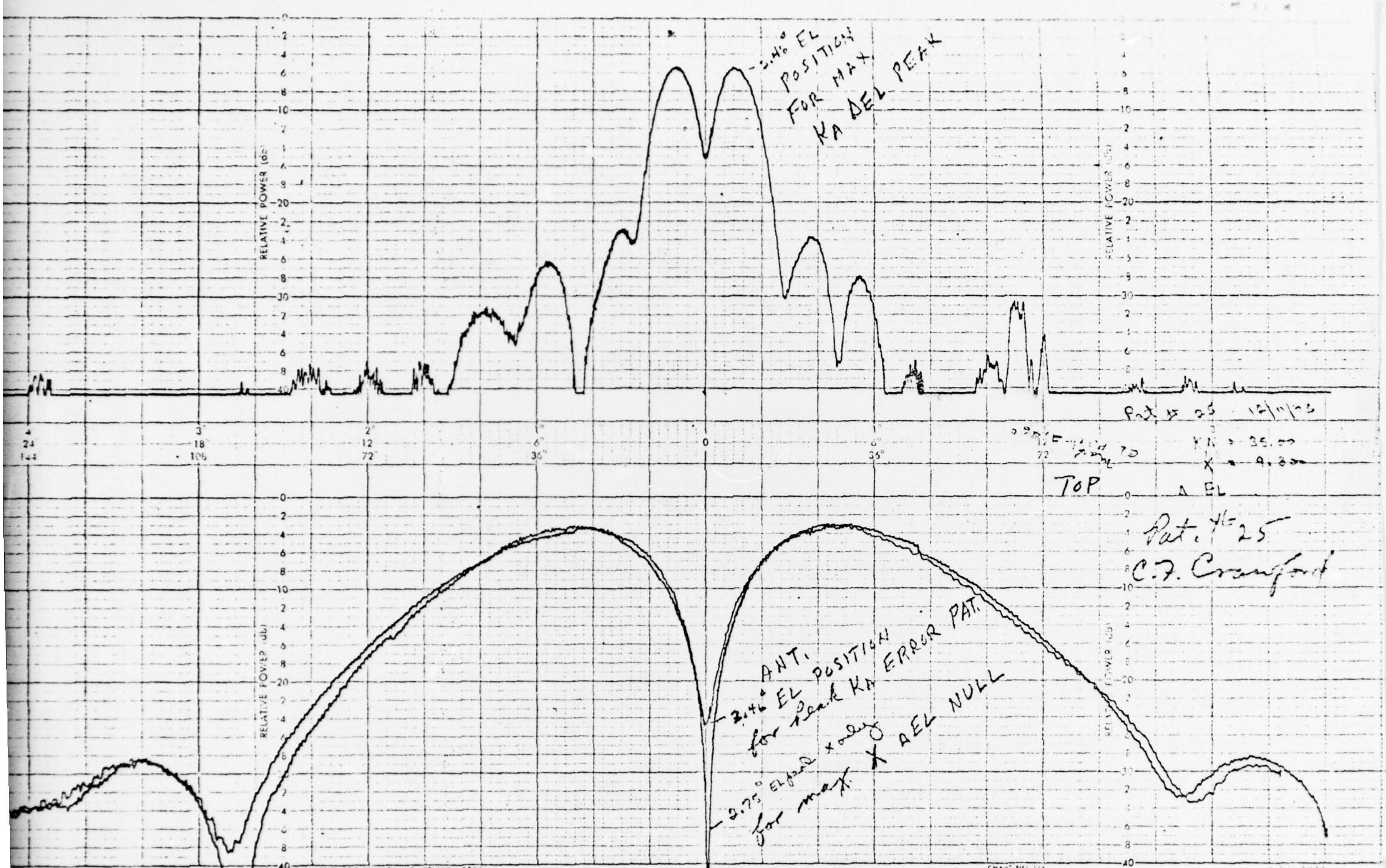
RELATIVE POWER (dB)
3.46° EL POSITION FOR MAX. KA ΔEL PEAK
Pat # 25 12/11/73
TOP
Δ EL
Pat. # 25
C.J. Crawford
ANT. 3.46° EL POSITION for peak KA ERROR PAT.
3.75° EL for max. X ΔEL NULL
SCIENTIFIC ATLANTA INC., ATLANTA, GEORGIA
CHART NO. 120